AD

Technical Report ECOM 2-66R-A

WATER TRANSFER FROM SOIL TO THE ATMOSPHERE

AS RELATED TO SOIL PROPERTIES, PLANT CHARACTERISTICS AND WEATHER

Annual Report
Cross Service Order 2-66
Task No. IVO-14501-B53A-08

Prepared by

S. L. Rawlins, Principal Investigator, with the cooperation of M. Clark, E. M. Cullen, F. N. Dalton, E. J. Doering, C. F. Ehlig, W. R. Gardner, R. D. Ingvalson and J. D. Oster.

U. S. Salinity Laboratory
Agricultural Research Service
U. S. Department of Agriculture
Riverside, California

as Research Report No. 391

December 1966

Distribution of this document is unlimited.

ECOM

UNITED STATES ARMY ELECTRONICS COMMAND
ATMOSPHERIC SCIENCES LABORATORY, RESEARCH DIVISION
FORT HUACHUCA, ARIZONA

Technical Report ECOM 2-66R-A December 1966

WATER TRANSFER FROM SOIL TO THE ATMOSPHERE AS RELATED TO SOIL PROPERTIES, PLANT CHARACTERISTICS AND WEATHER

Annual Report
Cross Service Order 2-66
Task No. 1V0-14501-B53A-08

Prepared by

S. L. Rawlins, Principal Investigator, with the cooperation of M. Clark, E. M. Cullen, F. N. Dalton, E. J. Doering, C. F. Ehlig, W. R. Gardner, R. D. Ingvalson and J. D. Oster.

U. S. Salinity Laboratory
Agricultural Research Service
U. S. Department of Agriculture
Riverside, California

as Research Report No. 391

for

U. S. Army Electronics Command
Atmospheric Sciences Laboratory, Research Division
Fort Huachuca, Arizona

SUMMARY

Application of the theory for thermocouple psychrometers developed in last year's report has led to construction of a psychrometer that essentially eliminates the requirement for precise temperature control. Psychrometers of this type were used to instrument a soil-plant system, and preliminary data on the influence soil-water potential on transpiration rate were collected.

In another experiment, a single pepper plant was grown in each of two soil columns 30 cm in diameter and 260 cm deep. A water table was set up in column A and the amount of water taken up from the water table was monitored daily. Column A received an amount of water approximately equal to 85% of that transpired since the previous irrigation. Column B received water equal to about 115% of the amount transpired. Soil water suction measurements were made daily with tensiometers placed at 50-cm depth intervals and at the 25-cm depth in the columns. Transpiration from the columns was determined daily by means of a load cell weighing system. Mathematical analysis of the data has not been completed, but an outline of the approach is given. It is apparent that attempts to estimate transpiration by means of soil moisture measurements will be in error if no way is provided to account for the flux of water into or out of the root zone.

The report includes the following chapter topics: plant-soil-water energy relations; water movement in the soil and uptake by plant roots; and further tests of the salinity sensor. Appendixes deal with psychrometric measurement of soil water potential without precise temperature control; design criteria for Peltier-effect thermocouple psychrometers; effect of soil salinity on water potentials and transpiration in pepper; and apparatus for weighing the long soil columns.

TABLE OF CONTENTS

INTRODUCTION

This report covers research work carried out by members of the staff of the U. S. Salinity Laboratory during the year ending June 30, 1966, under the Interdepartmental Cross Service Order, Fort Huachuca, Arizona - ENERGY BALANCE STUDIES (U. S. Army Electronics R & D Activity Task IVO-14501-B53A-08). It is the purpose of this research to describe the interrelation of the major factors determining the transfer of water from the soil to the atmosphere. Studies at this location emphasize the uptake of water from the soil by plants and are directed towards the development of a physical and mathematical model for this process which will lend itself to combination with models being developed elsewhere for the transpiration of water from plants.

During the past year continued emphasis has been directed towards improved methods of measuring the energy status of soil and plant water, and a better understanding of the movement of water within and below the root zone. These subjects are treated in the main chapters and in the first two appendixes. Appendix C treats the case where soil salinity contributes significantly to plant water potential which influences the rate of resulting exchange of water between the plant and the atmosphere. As in previous reports the first three appendixes are preprints of papers submitted for publication in scientific journals. Appendix D describes a weighing apparatus for large soil columns.

Several personnel changes have occurred during the past year. Dr. L. A. Richards and Dr. W. R. Gardner, Physicists, are no longer associated with the project. Dr. J. D. Oster, Physical Chemist and Mr. R. D. Ingvalson, Chemist, have joined the project.

CHAPTER I

PLANT-SOIL-WATER ENERGY RELATIONS

S. I Rawlins, W. R. Gardner and F. N. Dalton

Application of the theory for thermocouple psychrometers developed in last year's report has led to the construction of a psychrometer for field use that essentially eliminates the requirement for precise temperature control. A report on the theoretical principles involved in its development as well as details of construction and typical test data are included in Appendix A. This instrument has extended the range of our capability for measurement of water potential in the field from less than 1 bar (with tensiometers) to at least 40 bars. Our inability to measure water potentials in the field beyond the tensiometer range has seriously limited studies of water flow previously reported.

As a result of this development, we were able to instrument a soil-plant system in the greenhouse sufficiently well to collect some preliminary data on the influence of soil-water potential on transpiration rate. The same plant-soil system as described in Appendix A was used. Soil-water potential was measured at the 25-cm depth with a thermocouple psychrometer; leaf thickness was recorded continuously with a beta-ray attenuation apparatus similar to that reported by Gardner and Nieman in Appendix B of the 1964 Annual Report ERDAA Task 1-A-0-11001-B-021-08/02 (also now published in Science 143: 1460-1462, 1964); and transpiration rate was followed by making periodic weighings of the entire plant-soil system. The transpiration rate of a similar pepper plant rooted in nutrient solution and placed adjacent to the test plant

was also measured so that changes in transpiration rate from the test plant induced by variations in weather conditions could be separated from the reduction in transpiration induced by decreasing soil-water potential.

An estimate of the plant-water potential was obtained from the leaf thickness data by the following technique. Relative water content was determined on leaves removed from the plant three or four times during each day.* From these data, a calibration curve between leaf thickness and relative water content was obtained so that the continuous record of leaf thickness could be converted to a continuous record of relative water content. A calibration between relative water content and leaf-water potential was obtained with thermocouple psychrometers in the laboratory starting with fully hydrated leaves in the psychrometer chamber and measuring water potential after each of several successive drying increments.

Figure 1 shows soil-water potential (Ψ - soil) measured with the psychrometer at the 25-cm depth, plant-leaf-water potential (Ψ - plant) as inferred from leaf thickness measurements, and weight of the soil column (soil wt.) for a typical irrigation cycle. The dashed line intersecting the soil weight line is the calculated soil weight that would have existed had transpiration not been impeded by limited soil water. This was obtained by determining the ratio of the rate of water

---

*The pepper plant had several hundred leaves and produced new leaves at approximately the same rate they were removed for relative water content measurements.

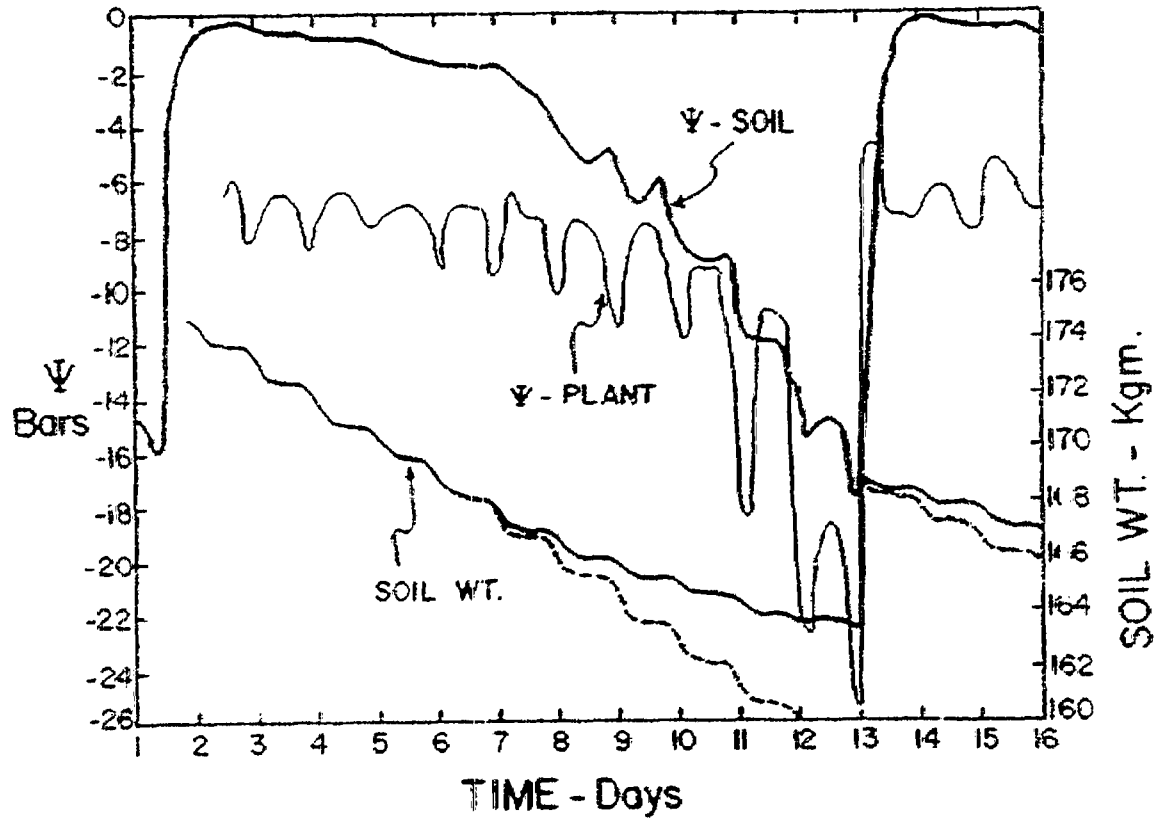

Figure 1.--Soil-water potential (Ψ - soil) measured with a psychrometer at the 25-cm depth, plant-leaf-water potential (Ψ - plant) as inferred from leaf thickness measurements, and weight of the soil column (soil wt.) for a typical irrigation cycle. The dashed line is the calculated soil weight that would have existed had transpiration not been impeded by limited soil water.

loss from the plant in the soil column to that of the plant rooted in nutrient solution at the time of maximum rate of loss from the soil column following irrigation. The dashed line was then calculated by subtracting the product of this ratio and the weight loss from the plant in nutrient solution from the soil weight.

The soil column was irrigated with 17 surface cm of nutrient solution on day 1 (1 March 1966), which brought the total weight of the column to about 175 kgm as shown. On day 2, tensiometers showed matric potentials of -0.025 bars at the 25-cm depth, and -0.05 bars at the 50-cm depth. The tensiometer at the 75-cm depth was off scale, indicating that the wetting front had not penetrated that deeply into the profile.

As water was extracted from the soil by evapotranspiration, the soil-water potential at the 25-cm depth (measured with the psychrometer) dropped gradually to -2 bars at day 7. At this time, the tensiometer at the same depth indicated a matric potential of only -0.4 bar. The osmotic potential of the nutrient solution used to irrigate the soil column was approximately -0.5 bar. For Pachappa soil, the water content at -0.4 bar is about half that at -0.025 bar. Thus, assuming that water was extracted by the plant roots at the 25-cm depth leaving all of the nutrient solute in the soil solution, the osmotic potential at this depth on day 7 should not have been lower than -1.0 bar. Adding the matric and the osmotic potentials on day 7, the total water potential should not have been lower than -1.4 bar. The lack of agreement between this value and the -2 bar value measured with the psychrometer is

approaching the precision of measurement with the psychrometer, but lag in the tensiometer readings caused by air accumulation in the tensiometer tube is probably a contributing cause to the deviation.

By day 8 following irrigation, the weight loss from the soil column each day was less than that calculated for a well watered plant as is shown by the difference between the solid and dashed lines for soil weight. This corresponds to the time when the plant-water potential began to fall below about -10 bars during midday. During days nine, ten and eleven, the plant-water potential fell several bars below the soil-water potential during the day, but recovered to approximately the value of the soil-water potential during the night. On day 12 the plant-water potential did not return to that of the soil during the night, indicating permanent wilting. This occurred at a soil-water potential of about -15 bars, which is considered to be the approximate wilting point based on standard wilting point determinations. By the time the permanent wilting point had been reached, the weight loss by the plant each day was reduced to less than 10% of its initial value. This is approximately the amount of water loss generally attributed to cuticular transpiration, indicating that the stomates were continually closed.

On day 13, the plant was irrigated with 6 liters of water. The recovery of water potential in the plant was almost immediate. The lag in rise of soil-water potential resulted from the time required for the wetting front to reach the 25-cm depth in the soil column. However, the transpiration rate did not resume its maximum rate, as is shown by the difference between the solid and dashed lines for soil weight for days 13

through 16. The reason for this lag in transpiration even though the plant had regained full turgor is not apparent. Further resolution of this point will require more complete instrumentation of the system.

CHAPTER II

WATER MOVEMENT IN THE SOIL PROFILE AND UPTAKE BY PLANT ROOTS

W. R. Gardner and E. M. Cullen

Greenhouse Experiments

Previous experimental and theoretical studies have dealt in part with the vertical movement of water within the soil profile. Analysis of the hydraulic head data from the field plot experiments of the last two years presented difficulties because of the lack of an independent measure of the flux of water across the 2-meter depth. To study this problem two large experimental soil columns were set up in the greenhouse. These were each 30 cm in diameter and about 260 cm in depth. This apparatus was designed and constructed under the supervision of E. J. Doering. A description is to be found in Appendix D of this report.

A single pepper plant was transplanted into each column. After the plants were well established in the columns the irrigation treatment was started. Each column was weighed daily by means of the load cell weighing system in order to determine the transpiration. Soil suction measurements were made daily at 50-cm depth intervals as well as at the 25-cm depth. Whenever the tensiometer at the 25-cm depth reached a suction of about 600-800 millibars, the plant was irrigated. Column A was irrigated with an amount of water approximately equal to 85% of the water transpired since the previous irrigation. Column B was irrigated with 115% of the amount of water transpired. A water table was set up at the bottom of column A in such a way that the water taken up from the water table could be monitored daily. The outflow from the bottom of column B was also recorded

daily. After about two months, a steady state was achieved at the bottom of the columns.

Hydraulic head data for a typical irrigation cycle for column A are shown in Figure 1. The average transpiration rate over several cycles for column A was 1.13 cm/day. Of this, about 1.0 cm/day was supplied by surface irrigation. The remaining 0.13 cm/day came from the water table below. It turned out that this 0.13 cm/day was very nearly the maximum rate at which water can be moved upward from that depth for the Pachappa soil used in the experiment. This was learned in later experiments in which a greater degree of under-irrigation resulted in a progressive drying of the soil profile, with a consequent failure to maintain a steady state.

Hydraulic head data for a typical irrigation cycle for column B are shown in Figure 2. The average transpiration rate in this case was 1.30 cm/day. The irrigation rate was 1.45 cm/day resulting in a leaching or drainage rate of 0.15 cm/day. The reason for the greater rate of transpiration from the plant in column B than from that in column A may have been its slightly larger size.

Figures 1 and 2 illustrate two important points. The hydraulic head patterns for the two columns are very similar in the top 75 cm. In that region, it is virtually impossible to tell from the data whether the irrigation rate is less or greater than the transpiration rate. It is only by looking at the direction of the water moving gradient below the root zone at about the 1-meter depth (or greater) that the direction of water movement is apparent. The second point, which was also borne

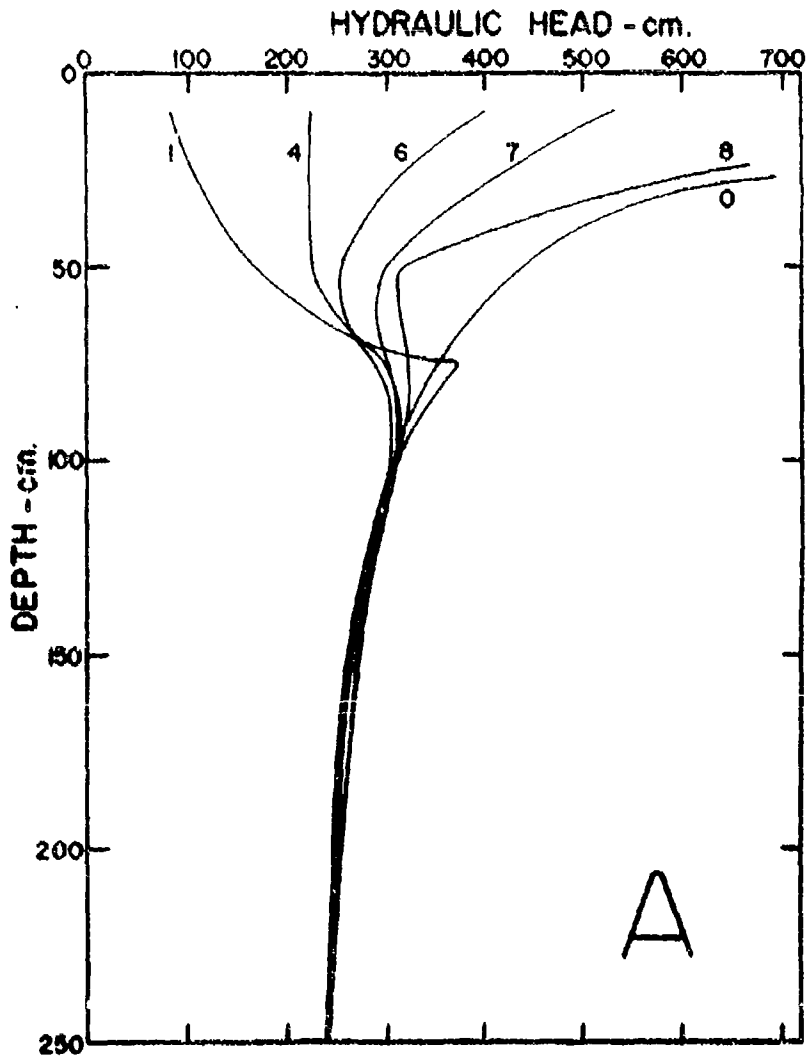

Figure 1.--Hydraulic head as a function of depth in soil column containing a single pepper plant. Numbers on curves indicate days after irrigation. Transpiration rate exceeded rate of surface irrigation. (Hydraulic head is the sum of the matric suction at some point and the depth of the point below the soil surface.)

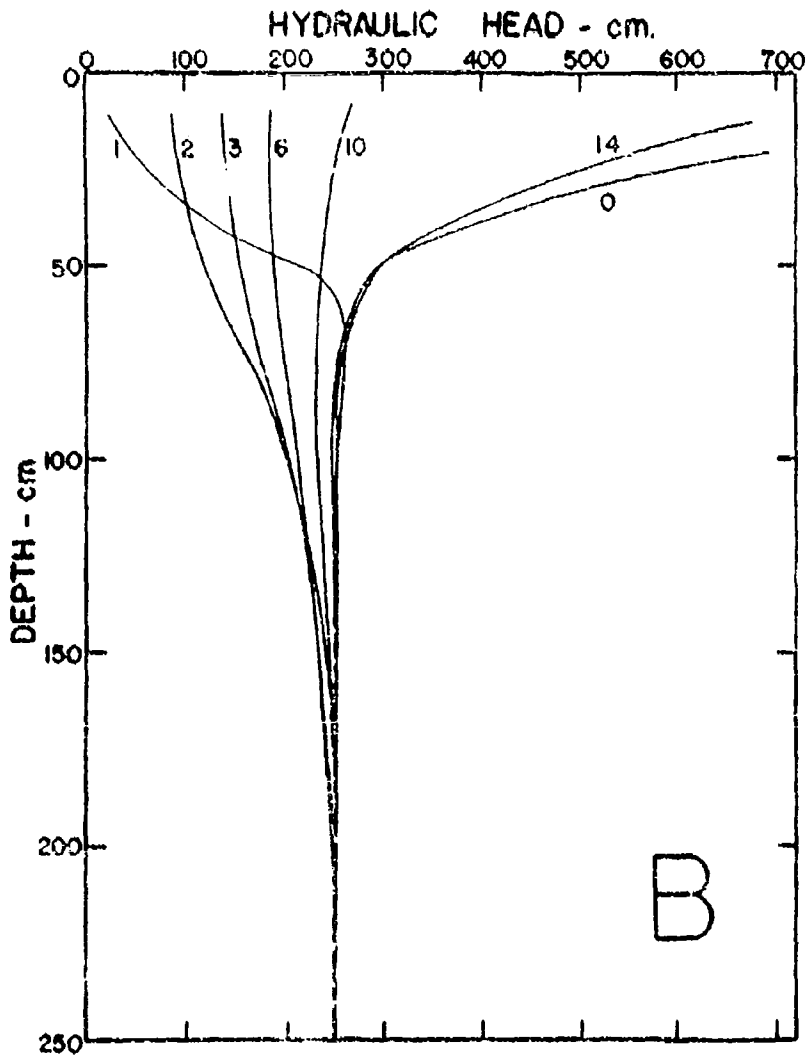

Figure 2.--Hydraulic head as a function of depth in soil column containing a single pepper plant. Numbers on curves indicate days after irrigation. Rate of surface irrigation exceeded transpiration rate. (Hydraulic head is the sum of the matric suction at some point and the depth of the point below the soil surface.)

out by the data from previous experiments, is that the fluctuations in the head imposed by the flux in and out of the top of the column damp out fairly rapidly with depth. The amplitude should damp out roughly as $\exp [-z (\pi/DT)^{\frac{1}{2}}]$ where z is the depth, D is the soil water diffusivity and T is the period. In this case, T is about 14 days for column B and 10 days for A. For column A, the suction is 200 millibars or more most of the time in the top meter, corresponding to a value for D of about 100 cm^2/day. This gives a 340-fold reduction in amplitude from the surface to 1 meter. Since column B is at lower average suction, it has a higher diffusivity and the wave is damped much less. This is accentuated by the fact that the diffusivity increases with depth. At the 150-cm depth, the diffusivity is about 500 cm^2/day. Hence, the amplitude at the 150-cm depth is roughly 1/25th of that at the surface. These are only order of magnitude estimates since they assume sinusoidal fluctuations and a constant diffusivity.

It is quite apparent that attempts to estimate transpiration by means of soil water content measurements will be in error if there is appreciable flux into or out of the root zone. Such attempts are especially subject to error when there is a net downward flux of water.

Mathematical Analysis of Experimental Data

The mathematical analysis of the data obtained in the large column experiments, as well as previous years' data, has not been completed. This is due, in the main, to the departure of Dr. Gardner from the project. This analysis is to be completed within the coming year and will be issued as a special report. Hence, only the brief outline of the approach

will follow. Supporting data and specific examples will be contained in the final report.

It should be stated at the outset that completely adequate quantitative theory for water uptake by plant roots does not yet exist. Inspection of the experimental data has led to certain simplifying assumptions which seem reasonable but which are semi-empirical and are not wholly satisfactory. It is quite apparent that further, and much more precise, experiments will be necessary, particularly in order to characterize the plant root system.

Steady-State Case

We consider first the steady-state case in which water is being added continually at a rate equal to or exceeding the transpiration rate, which is assumed to be constant. The flow equation then becomes

$$\frac{\partial \theta}{\partial t} = \frac{\partial}{\partial z}\left(k \frac{\partial H}{\partial z} \right) - Q(z) \qquad [1]$$

where H is the hydraulic head, z is the depth, k is the capillary conductivity and Q(z) is the rate of water uptake by the plant roots per unit volume of soil. The problem is to know what to write for Q(z) since we have reason to expect it to be a function of the root distribution and the hydraulic head in the plant as well as the hydraulic head in the soil. Examination of experimental data leads to the somewhat surprising conclusion that Q(z) = constant is as good an assumption as any, so far as the precision of the data are concerned. We therefore take $Q = E/L$, where E is the transpiration rate and L is the depth of the root zone. Since we are assuming steady state, $\partial\theta/\partial t = 0$. In order to integrate [1],

we must know the dependence of k upon depth. In a few special cases, k may be assumed to be reasonably constant, then:

$$H = H_o - z/k\,[I - (Ez/2L)] \qquad [2]$$

where I is the irrigation rate and H_o is the head at the soil surface. If k is taken as a function of the suction instead of being constant, the integration of equation [1] will usually require numerical methods. We see that k will be nearly constant if the suction does not vary greatly throughout the root zone. This requires that $(H - H_o) \approx L$, so that $k \approx (I - E/2)$. If $I = E$, then $k \approx E/2$. For reasonable values of E, this restricts k to 0.2 cm/day or greater. For Pachappa sandy loam, this corresponds to suctions less than 150 millibars.

Equation [2] is valid for the root zone. Below the root zone, $Q = 0$ and H is given by

$$H = H_o - \frac{1}{k}\left\{ z(I - E) - \frac{LE}{2} \right\}. \qquad [3]$$

If the water table is sufficiently deep, the soil suction below the root zone will be constant for a considerable depth and the hydraulic gradient will be unity. The water content of the soil will adjust itself so that k is equal to the flux (I - E), remembering that $I > E$.

Periodic Boundary Conditions

The actual field situation is more nearly represented by a steady-state condition at the bottom of the root system, but with a periodic boundary condition imposed at the surface. The solution for periodic boundary conditions has been discussed already (see report for 1964).

Since the sum of two solutions of the flow equation is also a solution, we combine equations [2] and [3] with the solution for a periodic boundary condition to get an approximate solution of the real case. The approximate nature of this solution needs to be emphasized. It appears from a number of studies that the rate of uptake of water within the root system is not uniform with depth. At first it is the greatest near the soil surface, but then decreases with time as the soil suction goes up. Concomitantly, the rate of uptake at the lower depths increases. The apparent uniform uptake of water with depth in the experiments may be a consequence of the periodic fluctuation of the soil suction. Under truly steady-state conditions a quite different extraction pattern would be obtained. This point requires further study. Even so, the sum of the periodic solution and the steady state solution gives a reasonable approximation of the hydraulic head patterns actually observed.

Non-Steady-State Extraction

The non-steady-state extraction problem presents more difficulties than the steady-state because the sink function, Q, in equation [1] is dependent upon time, t, as well as depth. For some problems, a usable degree of approximation can be achieved by assuming that water extraction within a portion of the root zone is uniform and that all water below that portion moves according to the flow equation. This upper region does not include the entire root system, rather, only that part in which verticle water movement in the soil is negligible. How the uptake by roots below this depth is treated depends upon whether the irrigation rate, I, exceeds the transpiration rate, E, or, on the average, is less than E.

If there is a net flux through the root zone and this flux is increasing with time (but does not approach the saturated permeability of the soil in magnitude), we can assume, as a good first approximation, that the suction at the bottom of the root zone will decrease and the water content will increase in just such a way as to maintain the conductivity equal to the flux. This assumes that the water table is infinitely deep. If the flux is decreasing with time, but is at all times downward, we find that the water content of the soil profile will decrease. This may be misinterpreted as water extraction by the plant roots when it is actually drainage out of the soil profile. An approximate method of treating the drainage problem has been published (Gardner, W. R., Soil Sci. Soc. Am. Proc. 26: 129-132, 1962). If the flux decreases rather sharply, from one steady-state rate to a lower one, the approach to a new equilibrium condition will go approximately exponentially, if the change does not correspond to too large a change in diffusivity. In this case the mathematical equations are applied to the region below that in which water extraction by the roots occurs.

If the irrigation rate does not exceed the transpiration rate, there is a net flux upward into the root zone. Here we are faced with serious difficulties in treating the problem exactly because it is difficult to separate the total upward flux moving in the soil from that in the plant. To do so would require more precise values for the capillary conductivity than are now obtainable in large soil columns or in the field. Inspection of the experimental data suggests that, again as a first approximation, the root zone can be divided into two regions.

In one, the conduction of water is essentially by means of the root system. Below this region, water movement may take place in both the soil and the root system, but the two are treated together as a rather complex composite porous medium. It is assumed that so long as the water movement is always in the upward direction, the upward flux will be proportional to the potential gradient as measured in the soil. The net effect of the plant roots is to maintain the apparent diffusivity of this combined system more nearly constant than that of the soil itself. Below about 150 millibars suction, the soil appears to conduct most of the water. By the time the suction is 1 bar, the plant roots predominate. In between, both are important. We then apply equation [1] to the region below the major portion of the root system assuming a constant diffusivity. We don't really know what this diffusivity is, but we can set some limits on it since it must be greater than the soil water diffusivity alone. In our field experiments, we found it to be around 100 cm^2/day for alfalfa on Pachappa sandy loam.

We can now write expressions for the amount of water that can be taken up from below the root zone before the transpiration rate is reduced due to wilting.

If the soil profile is wet to an infinte depth, the decrease in water content at the bottom of the root zone during the drying period is given by

$$(\theta_o - \theta) = \Delta\theta = 2\, q \sqrt{t/\pi\, \bar{D}} \qquad [4]$$

where θ_o is the initial water content, θ is the water content at time t, $q = (E - I)$, and $\bar{D}$ is the weighted mean diffusivity. If we assume that

the plant wilts and q ceases to be constant when θ reaches some limiting value θ_f, then $\theta_f - \theta_o = \Delta\theta_m$ corresponding to a limiting time, t_m:

$$t_m = \frac{\pi \bar{D}}{4 q^2} (\Delta \theta_m)^2. \qquad [5]$$

The total amount of water available to the plant from below, before wilting, is simply qt_m, so

$$qt_m = W_m = \frac{\pi \bar{D}}{4 q} (\Delta \theta_m)^2. \qquad [6]$$

If the soil profile is finite in depth, or wet only to a finite depth, we have instead of [4]:

$$\Delta \theta = q (t/L + L/2\bar{D}), \qquad [7]$$

where L is the depth of wetting. For this case,

$$qt_m = W_m = (L \Delta \theta_m - qL^2/3\bar{D}). \qquad [8]$$

Equations [6] and [8] give the contribution to the evaporation from the region below the major portion of the root zone. The total evaporation is obtained by multiplying t_m by the evaporation rate E. If E is known but not q, an exact solution to the equation can be found quite readily. However, a series of successive approximations will do almost as well. Equation [7] is valid only for sufficiently large t or small L. In order to treat the system as finite, $L < 3\bar{D}\,\Delta\theta/2q$. When this criterion is not satisfied, equations [4], [5] and [6] should be used.

A word or two about the weighted mean diffusivity, D, is in order. In the absence of roots, this is a weighted average of the soil water diffusivity. For an infinite system, the weighting function has been

described in a Laboratory publication (Gardner, W. R. Solutions of the flow equation for the drying of soils and other porous media. Soil Sci. Soc. Am. Proc. 23: 183-187, 1959). For a finite system, this becomes very nearly the diffusivity at the bottom of the profile and cannot really be treated as a constant. This problem is essentially the same as that treated by Gardner and Hillel (J. Geophys. Res. 67: 4319-4325, 1962). In the presence of plant roots, the weighted mean diffusivity of the soil-root system appears to remain more nearly constant during a given drying cycle. Its value will depend upon both the soil and the plant root system. In the field experiments on alfalfa and birdsfoot trefoil at the Laboratory, values of the order of 400 cm^2/day seem to be reasonable. The diffusivity for the soil itself ranges from 400 cm^2/day at field capacity down to about 10 cm^2/day at wilting. For Pachappa sandy loam, $\Delta\theta$ is about 0.15.

CHAPTER III

FURTHER TESTS OF THE SALINITY SENSOR

J. D. Oster and R. D. Ingvalson

The preliminary results of a study to determine the effectiveness of the salinity sensor in measuring the electrical conductivity of the soil solution at various depths in the root system of a plant are reported in this Chapter. Previous work was reported by L. A. Richards in Appendix C, Annual Report ERDAA Task 1-A-0-11001-B-021-08, July 1965 (also now published in Soil Sci. Soc. Am. Proc. 30: 333-337, 1966) in which it was shown that the salinity sensor appeared to give reasonable values for the electrical conductivity of the soil solution in a simulated root environment. Sensors used in our study were made according to the specifications given by Richards, with the exception that the ceramic was fired for four hours at 1000°C instead of two. Special care was taken to select only those sensors whose front electrode was covered with a thin layer of ceramic.

The reciprocal of the resistance of the conductivity element of the sensor was calibrated against the electrical conductivity (EC) of standard KCl solutions. The resistance of the thermistor element was calibrated as a function of temperature. During the course of this study, the resistance of both elements was measured independently. The thermistor resistance was converted to temperature and the resistance of the conductivity element was then corrected to that at 25°C. The table on page 90 of U. S. Dept. of Agr. Handbook 60, Diagnosis and Improvement of Saline and Alkali Soils, was used to accomplish this correction.

A pepper plant was grown in a column of Pachappa sandy loam soil 29.5 cm in diameter and 173 cm in length. Tensiometers and extraction cups were installed at the 30-, 60-, 90-, 120-, and 150-cm depths and salinity sensors at the 20-, 30-, 40-, 50-, 60-, and 90-cm depths. The column was first weighed and then irrigated when the tensiometer at the 60-cm depth read 0.3 bar. The amount of water applied exceeded by 10% the amount evapotranspired. The chemical composition of the applied water, expressed in meq/liter was: Ca 9.0, Mg 6.0, Na 12.8, SO_4 12.9, Cl 8.2, HCO_3 6.7, which resulted in an electrical conductivity of 2.3 mmho/cm. The relationship between matric suction and water content (θ) was determined from gravimetric water content of soil samples taken at various depths and corresponding tensiometer data. The average bulk density (ρ) of the column was 1.67 gms/cm^3 calculated from the oven-dry weight of the Pachappa soil used to pack the column.

The date and amount of water applied is reported in Table 1 together

Table 1.--Estimated depth of penetration of the applied irrigation water.

Date of Irrigation	Equivalent surface depth applied (d)	Depth of penetration of applied water* ($d/\rho\theta$)
July	cm	cm
1	9.71	32 ±3
8	11.59	39 ±3
16	12.38	41 ±3

*The average matric suction was 93 mbar, at the 30-cm level 24 hours after application of water. This value of matric suction was used to estimate water content (18%) from water retention curves. The limits of error reflect the uncertainty in estimating the water content.

with an estimate of the depth to which this water penetrated in the column during the first 24 hours following irrigation. Also indicated is the possible error associated with this estimate, which results primarily from the uncertainty in estimating θ from the matric suction-water content relationship at low suction values. The estimate does not take into consideration the evapotranspiration by the plant during this interval of time. The average evapotranspiration rate was 1.3 cm/day or, based on .30 cm^3 H_2O/cm soil 24 hours after irrigation, an error in penetration of about 4 cm. Hence, the number reported may be too great but should serve as an approximate point of reference to predict the behavior of the sensors.

Using Table 1 and assuming piston displacement of solution from the soil, the sensors at the 20- and 30-cm depths should indicate the EC of the applied water 24 hours after irrigation. The sensor at the 40-cm depth may not be affected by the applied irrigation water, but rather may reflect the concentration of the soil solution above this depth before the irrigation was applied. This may not be the case for the last irrigation where the predicted depth of irrigation is 41 cm.

The electrical conductivity and matric suction as a function of depth and time are shown in Figure 1. Within 24 hours after the three irrigations, the sensor at the 20-cm depth indicated an EC of 1.7, 2.2, and 2.1 mmho/cm. The EC of the applied water was 2.3 mmho/cm, and, hence this sensor functioned as expected. During the remaining portion of the irrigation cycle, the EC increased with time, apparently in response to water uptake by the roots of the pepper plant. The sensor at the 30-cm

level responded in a similar manner. However, the EC 24 hours after irrigation was higher in every case than that of the irrigation water even though the depth of penetration predicted for each irrigation was greater than 30 cm. This would indicate considerable mixing of applied irrigation water and residual soil solution at this depth.

A sample of the soil solution was obtained at the 30-cm depth by vacuum extraction via the extraction cup. The EC of this sample was determined using a standard conductivity cell. The solid circles in Figure 1 represent the values obtained in this manner. The two methods agree within 0.5 mmho/cm.

Within eight hours of the second and third irrigation, the sensor at the 30-cm depth showed a marked increase in EC as can be seen in Figure 1. This corresponded in time to a rapid decrease in matric suction indicating the passage of a wetting front at this depth. The increase in EC reflects the downward displacement of salts concentrated at the surface of the soil due to evaporation.

At the 40-cm level, the first two irrigations resulted in a rapid increase in the EC in the first 24 hours followed by a slow increase with time. This is in agreement with the proposal that the irrigation water would not penetrate to this depth. The water penetrating this depth during the second irrigation cycle had approximately the same EC as the soil solution at the 30-cm depth prior to irrigation, indicating a downward displacement of the residual soil solution. This displacement reoccurred during the third irrigation cycle. From Table 1 we see that the predicted depth of penetration is 41 cm indicating that salts

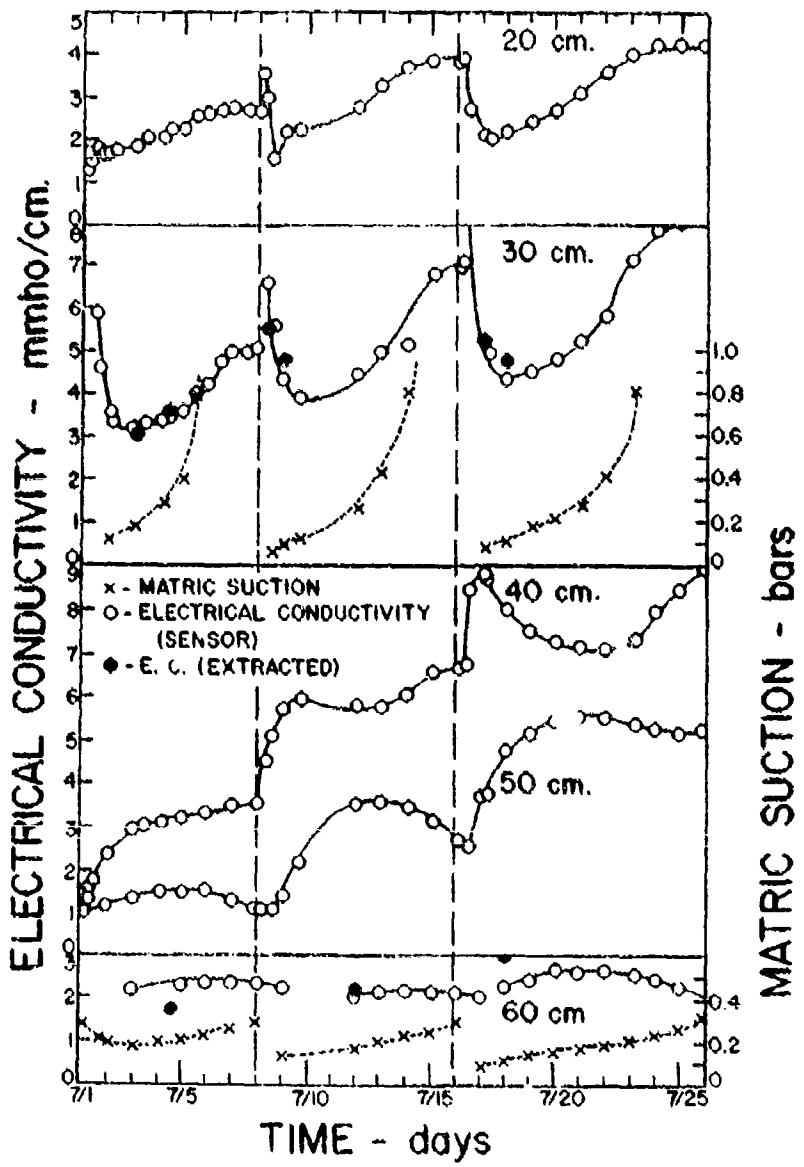

Figure 1.--Change in electrical conductivity and matric suction with time at several depths for three irrigation cycles in a column of Pachappa sandy loam containing a single pepper plant. The vertical dashed lines indicate the day of irrigation.

concentrated at the surface due to evaporation may penetrate the 40-cm depth. The more gradual decrease following the initial change in EC during the third irrigation cycle very likely results from some mixing of the concentrated soil solution with the applied irrigation water at this depth. This was followed by an increase in EC due either to water uptake by the roots of the plant at this depth or the more concentrated soil solution returning to this depth due to upward flow of water in the soil profile that began on the 19th. The direction of water flow was determined from the tensiometer data.

The EC at the 50-cm level first increased and then decreased in value during an irrigation cycle. The maximum values on the 12th and 22nd correspond in time to the change in direction of water movement in the profile between the 30- and 60-cm depths on the 11th and 19th. The increase in EC with time following irrigation indicates downward displacement of the more concentrated water between the 40- and 50-cm levels. Within three days after the direction of water flow changed in the profile, the EC began to decrease because of upward displacement of less concentrated water. The 60-cm sensor varied little during the course of the study reported, and the EC of the extracted soil solution at this depth is in fair agreement with that obtained from the sensor.

The EC as a function of depth during the three irrigation cycles is shown in Figures 2, 3, and 4. The curve drawn through the data on the 1st day of July formed the bases for the curves presented to connect the data for the 3rd, 5th and 7th. The maximum EC in the profile recorded on the 1st was assumed to be displaced downward with little

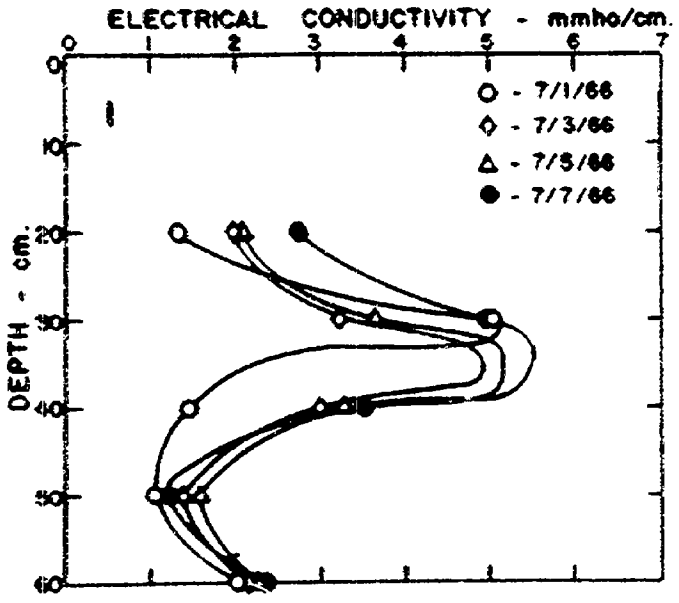

Figure 2.--Electrical conductivity as a function of depth (measured positively downward) and time for the first irrigation cycle shown in Figure 1.

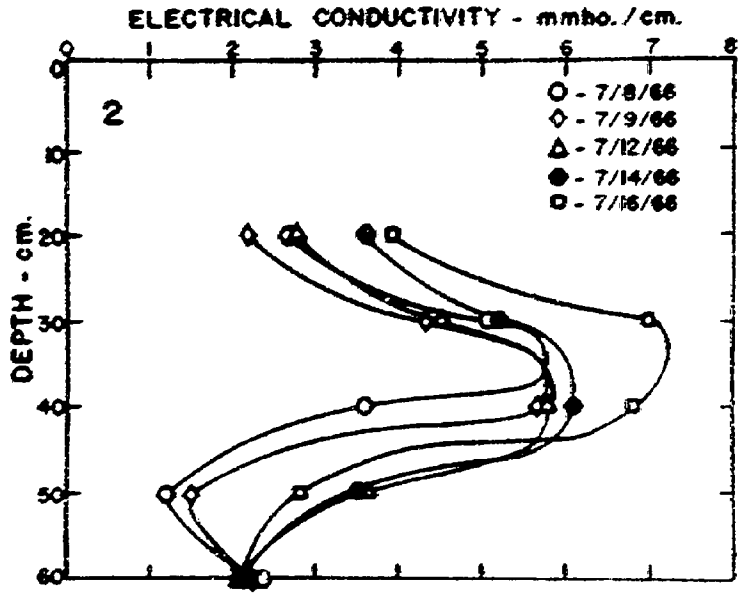

Figure 3.--Electrical conductivity as a function of depth and time for the second irrigation cycle shown in Figure 1.

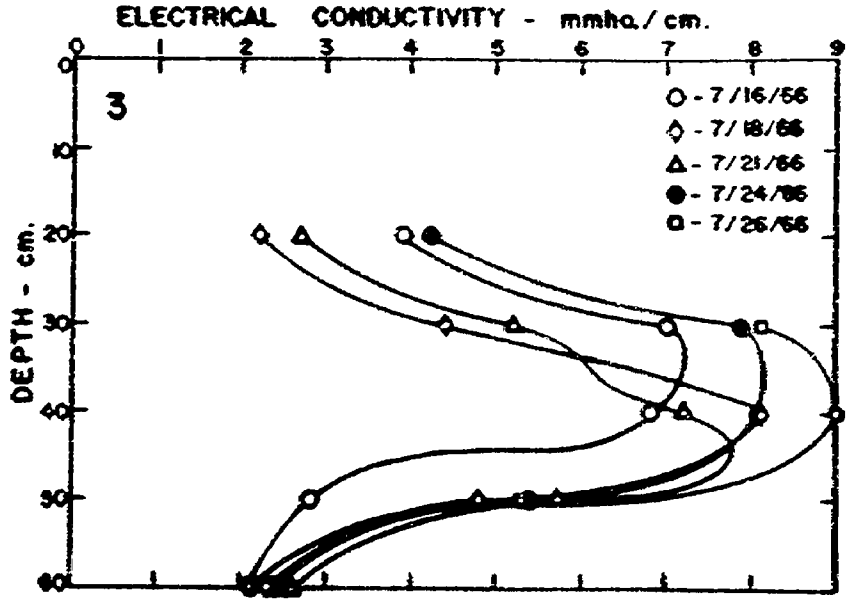

Figure 4.--Electrical conductivity as a function of depth and time for the third irrigation cycle shown in Figure 1.

change in maximum value or shape. The result is the curve drawn through the points on the 3rd. The curves on the 5th and 7th then follow and are based on the changes that occurred at the recorded depths, and reflect water uptake by the plant with an increase in EC between the 20- and 40-cm depth.

For the second irrigation cycle, Figure 3, the curve drawn through the values is very similar to that of the 7th in Figure 1. The same procedure as that explained above was used to connect the data points on the 9th, 12th, 14th and 16th. The curve of the 16th was repeated exactly in Figure 3, and the same procedure followed to draw the curves connecting the points. However, in this case, it appears the curve on the 16th was in error in that the EC at the 40-cm level on the 18th exceeded that of any value shown on the curve of the 16th. The opposite should be true considering that mixing of the applied water with the soil solution would cause the electrical conductivity to be less on the 18th than that on the 16th. If piston displacement without mixing of the two solutions is the method by which irrigation water penetrates a soil profile, then the curves should have the same maximum height.

Figures 2, 3, and 4 indicate that the EC can change very abruptly with depth, and that EC measured by each sensor appears to be correct when its values are compared to that of the sensors above and below it.

The predicted and measured values of the EC at the 20-, 30- and 40-cm depths at the end of the first and third irrigation cycles are given in Table 2. The predicted value is based on the assumption that the change in EC at some depth in the root system during an irrigation cycle is inversely related to the change in water content at that depth.

Table 2.--Predicted and measured values of the electrical conductivity at the 20-, 30- and 40-cm depths at the end of the first and third irrigation cycles.

Depth	Date	Water Content (θ)			Electrical Conductivity		
		Initial	Final	Ratio	Initial	Predicted	Measured
		gms H_2O / 100 gms soil		initial / final	mmho/cm		
cm	July						
20	3-7	13.5	6.6	2.0	1.9	3.9	2.7
	18-25	15.7	6.1	2.6	2.2	5.7	4.3
30	3-7	13.5	6.7	2.0	3.2	6.4	4.9
	18-25	15.7	6.5	2.4	4.4	10.6	7.8
40	3-7	13.5	8.7	1.6	3.0	4.6	3.5
	21-25	11.1	9.4	1.2	7.2	8.5	8.6

The initial and final EC values for each depth were obtained from Figure 1. The initial water content was estimated from the water retentivity curve and the matric suction at the 30-cm depth. The final water content was determined from soil samples taken on the 7th and 25th. With one exception, the predicted and measured values of EC differ with the measured values being smaller. This may be due to several causes, namely, 1) precipitation of salts in the soil solution, 2) dehydration of the sensor causing the resistance of the sensor to increase with a consequent decrease in the EC being read from the calibration plot of reciprocal resistance versus electrical conductivity, and 3) the inability of the sensor to remain in diffusional equilibrium with the soil solution when the soil becomes dry. If all the bicarbonate ions in the applied irrigation water (EC of 2.3 mmho) precipitated as calcium carbonate as the soil solution was concentrated twofold, the predicted EC would be too

high by about 1.3 mmho/cm [(2 × 6.7 meq/l) ÷ 10 meq/l/mmho/cm ≅ 1.3 mmho/cm]. This estimate could be high because work at this Laboratory shows that not all bicarbonate ions will precipitate (Bower and Wilcox, Soil Sci. Soc. Am. Proc. 29: 93-94, 1965). However, the initial EC values in Table 2 for the 30- and 40-cm depths are greater than 2.3 mmho/cm and as a result the concentration of bicarbonate ions will tend to compensate for the error made in assuming total precipitation. With one exception, the differences between the predicted and measured EC are less than 1.5 mmho/cm. The difference of 2.8 mmho/cm, during the third irrigation cycle at the 30-cm depth, may be a consequence of the high initial EC of 4.4 mmho/cm. Precipitation of calcium carbonate during an irrigation cycle may explain the differences between predicted and measured EC values. A more exact calculation of the amount precipitated and resulting change in EC to be expected could be made if the composition of the soil solution and atmosphere were more accurately known during an irrigation cycle. This work is currently in progress.

In conclusion, the sensors reflected changes in EC during an irrigation cycle due to water uptake by the root system of the plant, salt movement in the soil profile by convection with and diffusion in water and precipitation of salts.

PSYCHROMETRIC MEASUREMENT OF SOIL WATER POTENTIAL WITHOUT PRECISE TEMPERATURE CONTROL

S. L. Rawlins and F. N. Dalton

Soil Sci. Soc. Am. Proc. __: __-__, 1967.

APPENDIX A

USSL Publ. No. 435

PSYCHROMETRIC MEASUREMENT OF SOIL WATER POTENTIAL WITHOUT PRECISE TEMPERATURE CONTROL[1]

S. L. Rawlins and F. N. Dalton[2]

The inference of water potential from measurement of the equilibrium relative humidity of soil with a psychrometer offers several advantages over other methods. One of the most important of these advantages is that the theoretical relation needed to obtain water potential from relative humidity at any temperature can be derived with the only assumption being that water vapor behaves as an ideal gas. Since this assumption introduces negligible error in the vapor pressure range normally encountered, measurements of equilibrium relative humidity yield highly accurate estimates of water potential. Furthermore, since only a minute quantity of water is required to move from the sample to bring the psychrometer chamber to vapor equilibrium, the change in potential of the sample resulting from the measurement should be slight. The major difficulty with the technique arises from the fact that the change in relative humidity with water potential is small. For example, at 25°C. a change of water potential of 15 bars is accompanied by a change in relative humidity of about 0.01. Because the

---

[1]Contribution from the U. S. Salinity Laboratory, Soil and Water Conservation Research Division, Agricultural Research Service, USDA, Riverside, Calif. 92502. This work was supported in part by the Atmospheric Sciences Laboratory, Research Division, U. S. Army Electronics Command, Fort Huachuca, Arizona 85613.

[2]Research Soil Scientist and Physicist, respectively.

effect of temperature changes on relative humidity is often much greater than this, to measure only those changes in relative humidity resulting from changes in water potential, it has been necessary to control the temperature of the psychrometer chamber to within 0.001°C. or better. Unfortunately, this has precluded measurements of water potential in situ, except in rare cases in the laboratory. It is the purpose of this paper to explore possibilities for minimizing the effects of temperature changes on psychrometric measurements of water potential and to develop techniques to extend psychrometric measurements to the field.

Theory

Psychrometers used for measurement of water potential of soil samples consist of a sample chamber in which wet bulb temperature depression can be measured. Usually this wet bulb is one junction of a thermocouple with the reference junction at the wall of the sample chamber. The water potential of a sample is calculated from the temperature difference between these two junctions, given by the thermocouple e.m.f. With this arrangement, there are at least four ways in which changes in ambient temperature can cause changes in thermocouple e.m.f. with constant water potential in the sample.

The first of these arises from the fact that the theoretical relation between water potential and relative humidity is temperature dependent. At any given temperature, this relation is

$$\Psi = \frac{RT}{v} \ln RH \qquad [1]$$

where Ψ is the water potential, R is the ideal gas constant, T is the

absolute temperature, v is the volume of a mole of water, and RH is the relative humidity. Assuming, for the moment, that the thermocouple e.m.f. is a unique function of the chamber relative humidity, it is obvious, from the above equation, that the ambient temperature must be known to obtain the water potential from thermocouple e.m.f. This should cause little problem since it is only necessary to know this temperature within about 3°C. to infer water potential to the nearest percent.

The second way in which temperature affects the measurement of water potential with a psychrometer results from the fact that the relationship between wet-bulb depression and chamber relative humidity is temperature dependent. This effect, first reported by Klute and Richards (1962), is sufficient to cause errors in water potential of about 2% per degree centigrade. Change in psychrometer sensitivity with temperature can be explained on the basis of the temperature dependence of the thermal conductivity and water vapor diffusivity of the air in the chamber, and the heat of vaporization of water (Rawlins, 1966). Once the relation between psychrometer sensitivity and temperature is known, it should only be necessary to measure the ambient temperature to correct for this temperature effect.

The third effect of temperature to be considered arises whenever the chamber temperature differs from the temperature of the thermocouple reference junction. This can occur as a result of changing ambient temperature, which causes a temperature gradient between the outside and inside of the sample chamber. It can also be caused by heat production within the sample, as for example by respiration of plant tissue (Barrs, 1964). In either case, since the chamber and the reference junction are not at the same temperature,

the thermocouple does not measure the temperature depression of the wet-bulb below the chamber temperature as required. To correct for this, it is necessary either to measure the difference in temperature between the chamber and the reference junction, or to maintain the reference junction at chamber temperature. The latter course would be possible with thermocouples having a permanently wet junction, such as those developed by Richards and Ogata (1958). However, because of the high thermal conductivity of the copper wires by which this junction is connected to the measuring circuit, constructing it with fine enough wires to provide thermal isolation from the wall of the chamber has proved to be impractical. With thermocouples using Peltier cooling to condense water on the wet junction (Spanner, 1951), it is even less practical to maintain the reference junction at chamber temperature. Heat extracted from the wet junction during Peltier cooling flows to the reference junction and, therefore, must be conducted away from it if its temperature is to remain constant. Thus, it is necessary to connect the reference junction to a large thermal mass. With Peltier type thermocouples, however, the temperature difference between the chamber and the reference junction is easily obtained. This is given by the e.m.f. of the thermocouple before water is condensed on the wet junction. If this reference temperature remains constant during the cooling of the wet junction, it is only necessary to subtract the e.m.f. obtained prior to cooling from that obtained following cooling to obtain the e.m.f. resulting from depression of the wet junction temperature below the chamber temperature. If the difference in temperature between the chamber and the reference junction changes too rapidly with time to

consider it constant during the cooling period, it should be possible to estimate the temperature difference at the time the wet junction depression is measured by extrapolation of a curve of time versus temperature obtained immediately prior to cooling. If the temperature is varying rapidly, it is essential that the cooling period be kept to a minimum to avoid significant errors in estimating the chamber temperature. Since these errors contribute directly to error in estimation of the wet junction depression, and since the wet junction depression corresponding to 1 bar change in water potential is of the order of 0.01°C., precise measurements of chamber temperature are required.

Caution must be observed in using this technique to correct for elevations in chamber temperature caused by heat generation within the sample. Although the correct chamber relative humidity is obtained by this technique, this relative humidity will be that in equilibrium with the sample only if the chamber and the sample are at the same temperature. With sufficiently fine thermocouple wires (see Rawlins, 1966), heat flow to and from the chamber is essentially by radiation and conduction from the chamber wall. Therefore, if the sample covers the entire chamber wall, the temperature of the chamber will be the same as the sample. If only part of the wall is covered by the sample, the chamber temperature will be intermediate between the chamber wall temperature and the sample temperature. Thus, water evaporating from the sample is cooled as it enters the chamber, resulting in a higher chamber relative humidity than exists within the sample. The magnitude of the error in water potential resulting from this difference between sample and chamber temperature is the

same as that for uncorrected differences in temperature between the reference thermocouple junction and the chamber temperature.

In passing we point out that the technique of subtracting the e.m.f. measured prior to cooling the wet junction from that obtained following cooling not only corrects for temperature difference between the chamber and the reference junction, but also cancels any parasitic e.m.f.'s resulting from temperature differences between any other junctions in the thermocouple circuit. This greatly reduces the need for thermal grounding at junctions and terminals in the circuit normally required for low voltage measurements.

The remaining way in which temperature can cause errors in psychrometric measurements of water potential results from the fact that as air is heated its water vapor holding capacity increases. This causes a decrease in relative humidity unless sufficient water enters the air during heating to compensate for this increased water holding capacity. If a chamber were sealed so that water vapor could neither enter nor leave, the error in water potential resulting from changes in temperature of the chamber would be about 1 bar per 0.01°C at 25°C. If, on the other hand, vapor were free to move to and from the chamber from a sample, the error would be less. The error will be least in the case where the wet junction is completely surrounded by a sample with a wet surface, and where heat flow down the thermocouple wires to the chamber can be neglected. Under such conditions, the chamber temperature can change only as the sample temperature changes. But a change in sample temperature also causes a change in the vapor pressure within the sample. Thus, both heat and water

vapor flow to and from the chamber along the same pathways as a result of temperature changes in the sample.

If at any temperature, the latent heat of vaporization for water in the sample is the same as that for pure water, the relative humidity adjacent to the sample should be invariant with temperature. This can be seen from the Clapeyron-Clausius equation in the form

$$p_2 = p_1 \exp\left[\frac{L}{R}\left(\frac{T_2 - T_1}{T_2 T_1}\right)\right] \qquad [2]$$

where p_1 and p_2 are the vapor pressures at temperatures T_1 and T_2, L is the latent heat of vaporization of water, and R is the ideal gas constant. If L is the same for the water in the sample as for pure water, both the vapor pressure of water in the sample and the saturation vapor pressure resulting from a temperature change are obtained by multiplying the respective initial vapor pressures by the same factor. Since relative humidity is the ratio of these two pressures, the multiplying factor cancels, leaving the relative humidity unchanged by the temperature change. Available data (see for example Mooney, Keenan and Wood, 1952) show that for relative humidities above about 0.95, the latent heat of vaporization of water adsorbed on clays is essentially the same as that of pure water. The same holds true for solutions of salts commonly found in soils that are sufficiently dilute to maintain an equilibrium relative humidity above 0.95.

If, contrary to the assumption made above, there is a resistance to water movement between the chamber and the sample, significant errors in measurement of water potential could result from changes in temperature.

By differentiating equation [2], the change in vapor concentration in the chamber necessary to maintain constant relative humidity at 25°C. can be shown to be about 1.3 $\mu gm/cm^3$ for each degree change in temperature. The resistance to water flow between the chamber and the sample must be kept low enough that this flow of water does not result in a significant potential drop. For a spherical chamber of 1 cm. radius, whose wall separates the sample from the chamber interior, the flux of water per unit area through this wall necessary to maintain equilibrium will be about 0.4 dT/dt ($\mu gm/cm^2$ hr.), where dT/dt is the rate of temperature change. To maintain a water potential difference of less than 0.1 bar between the chamber and the sample, the conductivity of this wall must be at least 4 $\mu gm/cm^2$ bar hr. for each degree per hour change in temperature. The saturated conductivity of porous ceramic used in tensiometers is about six orders of magnitude greater than this. Thus, even for high rates of temperature change, no significant difference in water potential should occur across such a chamber wall.

METHODS AND MATERIALS

The psychrometer shown schematically in Fig.. 1 was selected for testing in soil because of its low sensitivity to temperature changes in the laboratory. Temperature fluctuations of several degrees centigrade throughout the day caused errors of less than 0.1 bar in chambers containing salt solutions of fixed water potential. The essential parts of the psychrometer are a porous ceramic bulb, whose primary function is to maintain a chamber of fixed dimensions within the soil, and a thermocouple to measure the relative humidity within the chamber.

The following procedure was used in constructing the psychrometer: (Numbers in italics refer to numbered parts in Fig. 1.) After machining and boring the Teflon insert 1, two copper heat sinks 2 were inserted as shown. The heat sinks used were copper electrical crimp connectors, but any small bore copper tubing would suffice. Their primary purpose is to provide sufficient thermal mass that their temperature remains essentially constant while the cooling current is passed through the thermocouple. Notches were cut at the tops of these heat sinks with a fine jewelers saw to form tieing posts for the thermocouple wires. A fine gauge hypodermic needle was used to make holes below each heat sink in the Teflon insert for the thermocouple wires 3. These wires (0.0025 cm. diameter Chromel-P and constantan from Omega Engineering[3], Springdale, Conn.) were inserted from the bottom side through the heat sinks and were mechanically secured by taking several wraps around the tieing posts. After inserting the copper lead wires 4, the heat sinks were soldered with cadmium-tin "low thermal" solder, using stainless steel solder flux. The entire assembly was then boiled in distilled water to remove any traces of flux and allowed to dry completely. A short length of acrylic tubing 5 was placed around the Teflon insert to serve as a handle and also to provide a container for the epoxy resin 6 used to encapsulate the heat sinks.

---

[3]The company names are included for the benefit of the reader and do not infer any endorsement or preferential treatment of products listed by the U. S. Department of Agriculture.

After the epoxy was set, the thermocouple assembly was calibrated as described below, and was then inserted into the neck of the ceramic bulb 7 and sealed with epoxy resin.

A diagram of the circuit used for cooling the wet junction and subsequently measuring the thermocouple e.m.f. is shown in Fig. 2. The connections and switches shown inside the dashed lines were mounted in an insulated aluminum box to prevent rapid temperature fluctuation at these junctions. The 4-pole, 2-throw switch is used to connect the thermocouple to either the voltmeter or the cooling circuit. It also short circuits the terminals of the voltmeter when the thermocouple is connected to the cooling circuit. This is an ordinary wafer switch, and thus gives rise to parasitic e.m.f.'s. These are easily cancelled by subtracting the e.m.f. prior to cooling from the final e.m.f. as discussed above.

The electronic voltmeter used was a Keithley Model 148 nanovoltmeter[3], which has a minimum range of 0.01 μv. This instrument is particularly useful for field applications because it is battery operated. The ammeter (50 milliamp), dry cell (1.5 volt) and variable resistor make up the cooling circuit. This is connected through a 2-pole, 2-throw polarity switch that reverses the current through the thermocouple to provide either cooling or heating of the junction.

The thermocouple was calibrated prior to sealing it into the ceramic bulb by mounting it in chambers of similar size that were lined with filter paper moistened with various concentrations of KCl solution. This was repeated at several temperatures to establish the temperature dependence of these calibration curves.

The procedure used to make a psychrometer reading was as follows: 1) The voltmeter was zeroed with its self-contained bucking voltage circuit; 2) The measuring junction was cooled by passing a 3 ma current through it for either 10 or 20 sec.; 3) The maximum thermocouple e.m.f. obtained after switching the thermocouple back to the voltmeter was recorded; 4) With the polarity of the cooling circuit reversed, a 3 ma current was passed through the thermocouple for about 20 seconds to heat the measuring junction and drive off any residual water. At water potentials below about -10 bars a 20-second cooling period was required to condense sufficient water to make measurement of the wet-bulb depression practical.

For the experimental test the psychrometer and a glass bead thermistor were buried 25 cm. from the top and 10 cm. from the side of a column of Pachappa sandy loam soil, 150 cm. deep and 30 cm. in diameter. The column was placed in a greenhouse and a pepper plant was grown in it to provide a means of changing the soil water potential rapidly. A tensiometer was installed at the same depth in the soil as the psychrometer.

RESULTS AND DISCUSSION

Fig. 3 shows water potential measured with the psychrometer and with the tensiometer, and soil temperature measured with the thermistor as functions of time for two typical irrigation cycles. The data points for the psychrometer have been corrected for change in psychrometer sensitivity with temperature. The column was irrigated on day 0, at 1300 hours on day 4, and at 1200 hours on day 16. In addition, a small quantity of water was added on day 8 to keep the water potential high over the weekend when no measurements were taken.

The decrease in water potential with time as water was extracted from the soil by the plant appears to be realistic. The largest part of this decrease for any given day occurred between 1000 and 2200 hours, which corresponded to a lag of about 4 hours behind the period of maximum transpiration by plants in this same greenhouse. It is probable that most of this lag is accounted for by capacitance in the plant and unsaturated soil near the roots. The rapid rise in water potential following irrigation is evidence that the psychrometer measurements do not lag far behind the actual soil water potential.

Although the soil temperature fluctuated as much as 4°C. per day, this does not appear to have caused serious fluctuations in the water potential measurements. This is particularly evident from day 5 to day 9 where the water potential was decreasing slowly. During this period, the variation of water potential was within ±0.5 bars, and appears to be random rather than following the fluctuations in soil temperature. By taking the average of several measurements, it would appear possible to estimate the soil water potential with a precision of a few tenths of a bar. This insensitivity of the measurements to temperature fluctuations is evidence that the psychrometer design meets the essential requirement that heat and water vapor move to and from the psychrometer chamber in phase. Thus, the porous ceramic bulb, which is required only for protection of the thermocouple and maintenance of the cavity in the soil, apparently offers the same resistance to vapor movement as it does to heat flow.

The failure of the psychrometric measurements of water potential to agree with the tensiometer readings following irrigation is not fully

accounted for by the presence of solutes in the soil water. One possibility for this deviation is failure of the concentrated solution from the dry soil to completely diffuse out of the ceramic bulb in the period of time following irrigation. A more likely cause for this deviation, however, is that the zero intercept of the calibration curve for the psychrometer mounted in the ceramic bulb and buried in the soil was different from that obtained with the thermocouple mounted in the filter paper-lined chamber used for calibration. The fact that the difference between the psychrometer measurements and the tensiometer measurements remains nearly constant for six days indicates that lack of equilibrium between the solutes in the ceramic bulb and the soil solution was not the problem.

SUMMARY AND CONCLUSIONS

With a psychrometer designed to meet the requirements outlined in the above theoretical analysis, the effects of moderate temperature fluctuations have apparently been eliminated from measurements of soil water potential. This overcomes the major limitation of psychrometric techniques for measuring water potential. With this technique and with the availability of a portable electronic voltmeter suitable for measuring thermocouple e.m.f.'s with the required accuracy, the way appears clear for the extension of measurements of total water potential to the field.

ACKNOWLEDGMENT

The authors wish to acknowledge the help of Dr. L. A. Richards in suggesting the use of and constructing the ceramic bulb used to enclose the thermocouple.

LITERATURE CITED

1. Barrs, H. D. 1964. Heat of respiration as a possible cause of error in the estimation by psychrometric methods of water potential in plant tissue. Nature 203: 1136-1137.

2. Klute, A., and Richards, L. A. 1962. Effect of temperature on relative vapor pressure of water in soil: Apparatus and preliminary measurements. Soil Sci. 93: 391-396.

3. Mooney, R. W., Keenan, A. G., Wood, L. A. 1952. Adsorption of water vapor by montmorillonite. II. Effect of exchangeable ions and lattice swelling as measured by x-ray diffraction. J. Am. Chem. Soc. 74: 1371-1374.

4. Rawlins, S. L. 1966. Theory for thermocouple psychrometers used to measure water potential in soil and plant samples. Agr. Meteorol. (in press).

5. Richards, L. A., and Ogata, Gen. 1958. Thermocouple for vapor pressure measurement in biological and soil systems at high humidity. Science 128: 1089-1090.

6. Spanner, D. C. 1951. The Peltier effect and its use in the measurement of suction pressure. J. Exptl. Bot. 2: 145-168.

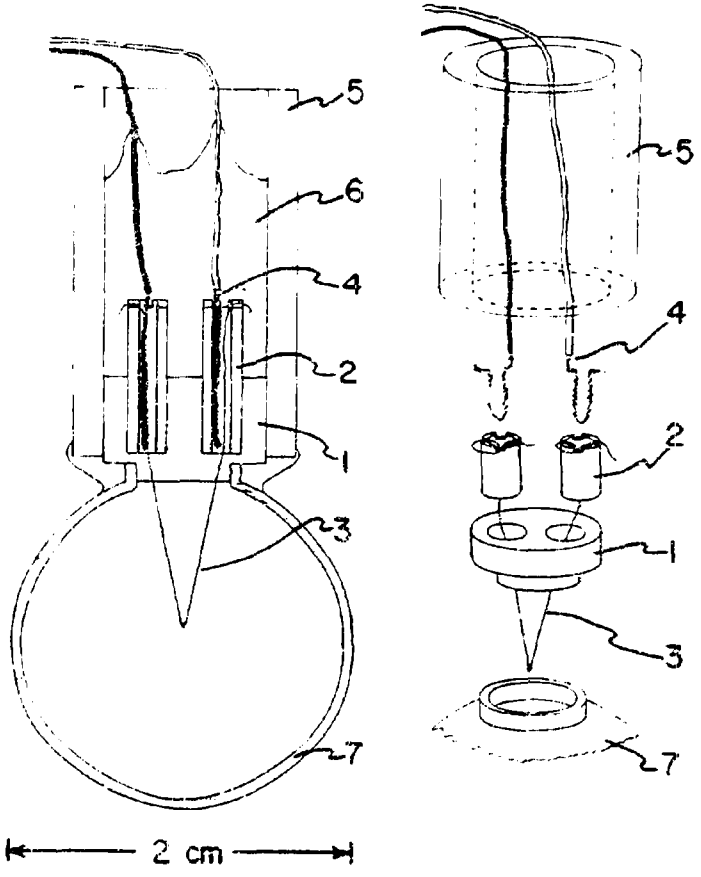

Figure 1.--Cross section and exploded view of the thermocouple psychrometer used for measuring soil water potential *in situ*.

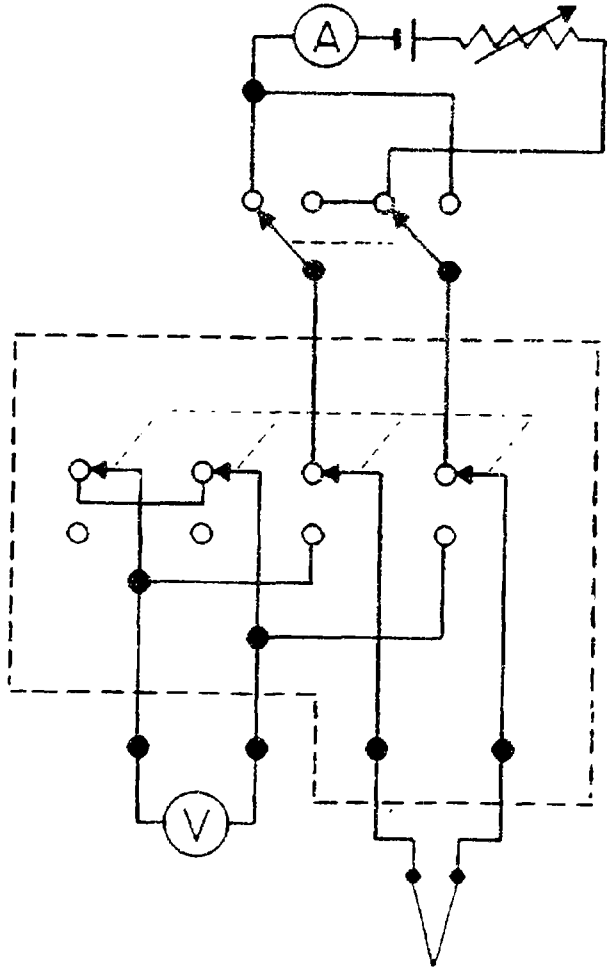

Figure 2.--Diagram of the electrical circuit for the thermocouple psychrometer

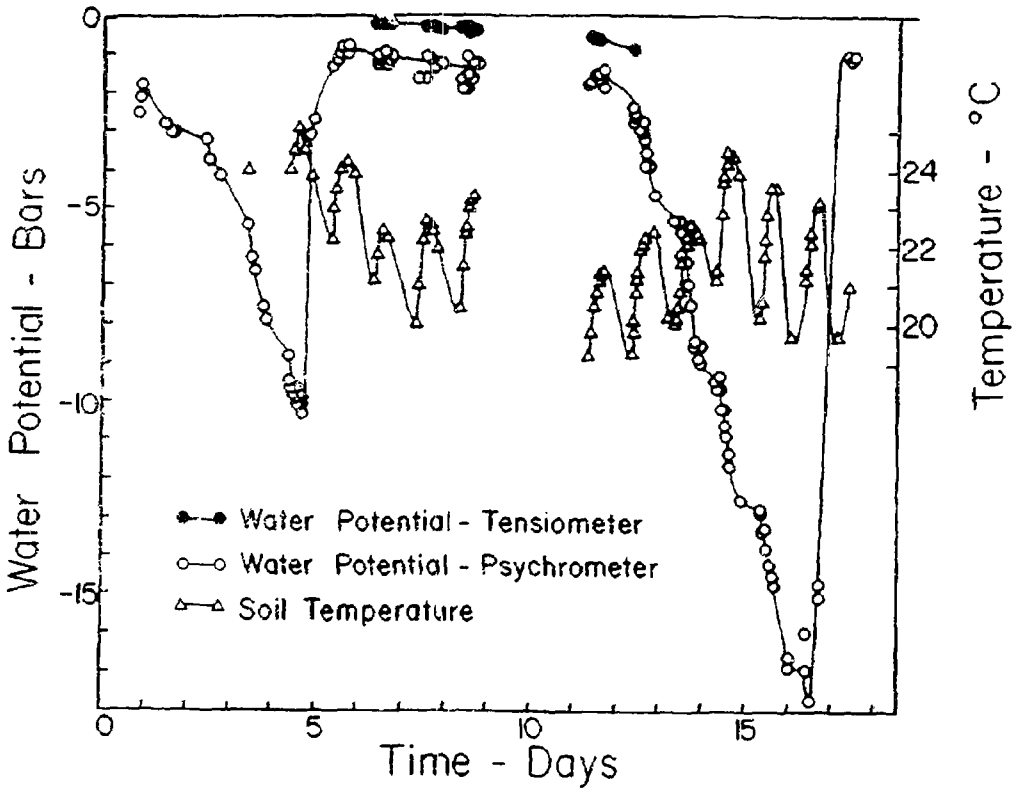

Figure 3.--Water potential as measured with a thermocouple psychrometer and with a tensiometer, and temperature at the 25 cm. depth in a soil column during two irrigation cycles.

APPENDIX B

DESIGN CRITERIA FOR PELTIER-EFFECT THERMOCOUPLE PSYCHROMETERS

F. N. Dalton and S. L. Rawlins

Soil Science ___: ___-___, 196_.

USSL Publ. #438

DESIGN CRITERIA FOR PELTIER-EFFECT THERMOCOUPLE PSYCHROMETERS[1]

F. N. Dalton and S. L. Rawlins[2]

[1]Contribution from the U. S. Salinity Laboratory, Soil and Water Conservation Research Division, Agricultural Research Service, USDA, Riverside, Calif. 92502. This work was supported in part by the Atmospheric Sciences Laboratory, Research Division, U. S. Army Electronics Command, Fort Huachuca, Arizona 85613.

[2]Physicist and Soil Scientist, respectively.

INTRODUCTION

Miniature thermocouple psychrometers that use the Peltier cooling effect to condense water on the wet junction have been developed to measure the relative humidity of air in equilibrium with soil and biological materials (1, 2, 4, 5, 6, 8). By this measurement, the energy status of water in these materials can be evaluated. In the past, the design of such psychrometers has relied heavily upon characteristics that are determined empirically. The two most common characteristics are the magnitude of the cooling current that gives the maximum temperature depression at the wet junction, and the heat capacity of the reference junction necessary to maintain its temperature within selected bounds during this cooling.

Spanner (8) developed equations governing optimum cooling current for such psychrometers, but his calculations were based on a requirement that the ratio of the radii of the wires of the thermocouple psychrometer be some constant. He also placed a similar constraint on the length of the thermocouple wires. In practice these constraints have been found impractical to meet, either because of geometrical limitations of the psychrometer chamber or because of the unavailability of thermocouples made from wires of different size. As a result, thermocouple psychrometers are usually constructed with the same dimensions for both metals making up the thermocouple.

In the derivation of the equations governing the optimum cooling currents and junction temperature depressions of Peltier-type thermocouple psychrometers, one must consider the rate at which heat is lost

from the surface of the thermocouple wires into the surrounding medium. For an increment of wire of length dx, the heat lost per unit area per second is given by (3)

$$Ha\theta dx \qquad [1]$$

where H is the heat transport coefficient, a is the circumference of the wire, and θ is the temperature difference between some point on the wire at position x and the surrounding medium. The generalized value of this heat transport coefficient takes into account all modes of heat transport, which, in the general case, are conduction, radiation, and convection.

Because the design of thermocouple psychrometers will undoubtedly vary depending upon application, it would be desirable to have a general equation from which critical design characteristics could be determined. It is the purpose of this paper to develop the equations governing optimum cooling currents and to present a method whereby the necessary heat transfer coefficient can simply be determined. The method herein described was used to obtain the heat transfer coefficient from fine wires in moist air; but it could be extended to deduce the thermal transport properties of porous media, liquids, and other gases. The mass of the heat sink at the reference junction of a Peltier psychrometer necessary to maintain the temperature within selected bounds during cooling of the measuring junction is also given as a function of the magnitude and duration of the cooling current.

THEORY

The differential equation relating the change in temperature of an electrically heated wire is:

$$KA\frac{d^2\theta}{dx^2} - Ha\theta - \frac{i^2\rho}{A} = 0 \qquad [2]$$

where K is the thermal conductivity of the wire, A is the cross sectional area, H is a heat transfer coefficient, a is the circumference of the wire, ρ is the electrical specific resistance, i is the current and θ is the temperature difference, from ambient, at some point x (3, 8).

The general solution to equation [2] is

$$\theta = Ce^{-\alpha x} + C'e^{\alpha x} - \frac{i^2\rho}{HaA} \qquad [3]$$

where $\alpha = \sqrt{Ha/KA}$.

In order to apply equation [2] to Peltier-type psychrometers, let two wires of radius r be joined at x = 0 to form a thermocouple junction. The subscripts 1 and 2 will be used to distinguish between the metals making up the bi-metallic junction.

At steady state, for semi-infinite wire, the boundary conditions determining C and C′ of equation [3] are (8),

$$\frac{d\theta}{dx} \to 0 \text{ as } x \to \infty \qquad [4]$$

$$-K_1 A \left.\frac{d\theta}{dx}\right|_{x=0} = \lambda_1 Pi \qquad [5]$$

where λ_1 is the proportion of heat being conducted down wire 1 toward x = 0, and P is the Peltier coefficient. If we let λ_2 be the proportion of heat being conducted down wire 2 toward x = 0, $\lambda_1 + \lambda_2 = 1$.

Solving for C and C′ and substituting into equation [3] gives for the temperature of wire 1,

$$\theta_1 = \frac{\lambda_1 P i}{\sqrt{K_1 A H a}} e^{-\alpha_1 x} - \frac{i^2 \rho_1}{H a A} \qquad [6]$$

A similar equation would hold for wire 2.

The current that causes the Joule heating to offset exactly the Peltier cooling at x = 0 can be found by setting the temperature depression θ equal to zero and solving for the current i. This leads to

$$i = \frac{\pi r^{3/2} \lambda_1 P \sqrt{2K_1 H}}{\rho_1 K_1} \qquad [7]$$

The current i can be determined experimentally with a milliammeter. Solving equation [7] for the heat transport coefficient H gives

$$H = \frac{K_1}{2r^3} \left(\frac{\rho_1 i}{\pi \lambda_1 P} \right)^2 \qquad [8]$$

Thus, the heat transport coefficient is given in terms of known parameters. λ_1 is determined under the constraint that $\theta = 0$ and that $i_1 = i_2$. To do this we use equation [7] to obtain

$$\frac{\pi r^{3/2} \lambda_1 P \sqrt{2K_1 H}}{\rho_1 K_1} = \frac{\pi r^{3/2} \lambda_2 P \sqrt{2K_2 H}}{\rho_2 K_2} \qquad [9]$$

Remembering that $\lambda_2 = 1 - \lambda_1$, equation [7] can be solved for λ_1 and λ_2

to yield

$$\lambda_1 = \frac{\rho_1 \sqrt{K_1}}{\rho_2 \sqrt{K_2} + \rho_1 \sqrt{K_1}} ; \quad \lambda_2 = \frac{\rho_2 \sqrt{K_2}}{\rho_1 \sqrt{K_1} + \rho_2 \sqrt{K_2}} \qquad [10]$$

For chromel-constantan thermocouples, the thermal conductivities are nearly equal, hence

$$\lambda_1 = \frac{\rho_1}{\rho_1 + \rho_2} ; \quad \lambda_2 = \frac{\rho_2}{\rho_1 + \rho_2} \qquad [11]$$

It must be remembered that the results given above are only valid under the constraint that the current is causing no temperature depression and that boundary conditions [4] and [5] are met.

For wires of finite length, L, equation [3] can be solved with boundary condition [5] and a new boundary condition

$$\theta = 0 \text{ for } x = L. \qquad [12]$$

Solving for C and C′ and substituting into equation [3] leads to the solution

$$\theta_1 = \frac{\lambda_1 \, Pi}{K_1 A \alpha_1} \frac{\sinh \alpha_1 (L - x)}{\cosh \alpha_1 L} - \frac{i^2 \rho_1}{HaA} \left(1 - \frac{\cosh \alpha_1 x}{\cosh \alpha_1 L} \right) \qquad [13]$$

where $\alpha_1 = \sqrt{Ha/K_1 A}$. This solution represents the temperature depression of the sensing junction of a thermocouple psychrometer in terms of the physical parameters of a single wire and the constant λ_1.

Now since $\theta_1\big|_{x = 0}$ must equal $\theta_2\big|_{x = 0}$, equation [13], evaluated at x = 0, and its equivalent with respect to wire number 2 can be equated.

Noting that $\lambda_2 = (1 - \lambda_1)$, one arrives at the expression

$$\lambda_1 P\left(\frac{\tanh \alpha_1 L}{K_1 \alpha_1} + \frac{\tanh \alpha_2 L}{K_2 \alpha_2} \right) - \frac{i}{Ha} \left(- \frac{\rho_1}{\cosh \alpha_1 L} + \frac{\rho_2}{\cosh \alpha_2 L} - \rho_2 + \rho_1 \right)$$

$$- \frac{P}{K_2 \alpha_2} \tanh \alpha_2 L = 0 \qquad [14]$$

This equation relates λ_1 and i when $\theta_1\big|_{x=0} = \theta_2\big|_{x=0}$. By using Lagrange's method of undetermined multipliers, with the constraining equation [14], equation [13] can be solved for the cooling current yielding maximum temperature depression at x = 0. This gives

$$i_{max} = P \pi r^{3/2} \tanh \alpha_1 L \tanh \alpha_2 L$$

$$\left\{ 2\sqrt{K_1 K_2} \left[\rho_1 \left(1 - \operatorname{sech} \alpha_1 L \right) \left(\frac{\tanh \alpha_1 L}{\sqrt{2 K_1 H}} + \frac{\tanh \alpha_2 L}{\sqrt{2 K_2 H}} \right) \right.\right.$$

$$\left.\left. - \tanh \alpha_1 L \left(\frac{\rho_1 (1 - \operatorname{sech} \alpha_1 L) - \rho_2 (1 - \operatorname{sech} \alpha_2 L)}{\sqrt{2 K_1 H}} \right) \right] \right\}^{-1} \qquad [15]$$

When $\alpha L > 5$, $\tanh \alpha L \to 1$ and $\operatorname{sech} \alpha L \to 0$ so that

$$i_{max} \cong \frac{P \pi r^{3/2}}{2\sqrt{K_1 K_2} \left[\left(\frac{\rho_1}{\sqrt{2 K_1 H}} + \frac{\rho_1}{\sqrt{2 K_2 H}} \right) - \left(\frac{\rho_1 - \rho_2}{\sqrt{2 K_1 H}} \right) \right]} \qquad [16]$$

Equation [16] corresponds to the optimum current when the boundary condition of a semi-infinite wire is met. For practical purposes, this occurs when $\alpha L > 5$. For wire of radius 0.00127 cm (1 mil diam.) $\alpha L > 5$ when $L > 0.8$ cm; for a wire of radius 0.008 cm (6.3 mil diam.) $\alpha L > 5$ when $L > 1.7$ cm.

EXPERIMENTAL SETUP

Figure 1 shows a schematic representation of the experimental setup used to determine the heat transport coefficient, H. Two chromel-constantan thermocouples of wire radius 0.00127 cm (1 mil diam.) were placed in an acrylic tube as shown. This tube was lined with filter paper saturated with a KCl solution having -10 bar osmotic potential. This was used instead of pure water to reduce the chance of vapor condensation on the thermocouple wires. The portion of the apparatus enclosed by the dashed line in figure 1 was placed in a thermostatic bath where the temperature was controlled to within $\pm\ 2 \times 10^{-4}$°C.

Current was passed through thermocouple A in such a direction to cause the junction J_a to be cooled. The current was adjusted with rheostat R and monitored by milliammeter M to within ±.05 ma. The temperature of junction J_a was monitored by thermocouple B. The voltage output of thermocouple B, which was as high as 30 microvolts, was measured with a high impedance volt meter with precision of $\pm 10^{-8}$ volts.

When a cooling current of small magnitude was passed through thermocouple A, thermocouple B registered a reduced temperature at junction J_b. As the cooling current was increased, the temperature depression at J_a reached a maximum, after which further increase in current caused Joule heating to increase more rapidly than Peltier cooling. The current could be increased to such a value that Joule heating fully compensated for Peltier cooling resulting in no temperature depression at the junction J_a. By determining the current that

causes the Joule heating to compensate exactly for the Peltier cooling at J_a, one can deduce the value for the heat transfer coefficient H, as is shown in the following section.

RESULTS AND DISCUSSION

Heat Transport Coefficient

Since heat loss can be due to a number of processes, the calculation of the heat transport coefficient from handbook data would be tedious and require a number of assumptions. Equation [1] states that the heat loss per unit area from the thermocouple wires is proportional to the first power of the temperature difference between the wire and the surrounding media. This of course is an approximation and is valid only for small temperature differences. Because radiation is one mode of heat transport, the value for the heat transport coefficient will be slightly dependent upon the emissivity of all surfaces exposed to the thermocouple wires. If relative humidity measurements with thermocouple psychrometers are taken in systems where the surface exposed to the thermocouple wires is wet, then the emissivity of this surface would not be different from that of the wet filter paper used in the experiment.

The boundary condition [5] would not be met if water vapor condensed on the thermocouple wires while the cooling current was being adjusted to give zero temperature depression at J_A. To circumvent this problem, we started the current at a sufficiently high magnitude to cause a temperature elevation at the sensing junction and then reduced it until zero temperature depression at J_a was observed.

After determining that a current of 5.90 ma. caused zero temperature depression, equation [7] was used to calculate a value for the heat transport coefficient. With K_1 = 0.22 watts/°C/cm, $\rho_1 = 49.0 \times 10^{-6}$ ohm-cm, $P = 18.03 \times 10^{-3}$ volts (at 25°C) and λ_1 = 0.41 (from equation [11]); H turns out to be 83.21×10^{-4} watts/cm^2/°C. Spanner reports a value of 12.4×10^{-4} watts/cm^2/°C. The effects of these two values on optimum cooling currents will be compared below.

Optimum Cooling Current

The calculated value for the heat transport coefficient was used in equation [15] to calculate the optimum cooling current for a Chromel-Constantan thermocouple as a function of the length and radius of the thermocouple wire with K_2 = 0.20 watts/°C/cm and $\rho_2 = 70.6 \times 10^{-6}$ ohm-cm. Figure 2 shows optimum cooling current versus thermocouple wire length for wires of various radii. The optimum cooling current increases with decreasing thermocouple wire length. For any given wire length, the optimum cooling current increases with increasing wire diameter, and for any given wire diameter there is a length beyond which there is no decrease in the optimum cooling current.

Table 1

Table 1 gives a comparison between empirically determined optimum cooling currents obtained from the literature, and those calculated from equation [15] for a temperature of 25°C. Both the value of H determined herein and that reported by Spanner were used. The agreement between the predicted and observed optimum cooling current for H calculated from equation [8] is excellent for wires of small radius. As the wire

Table 1.--Comparison of optimum cooling currents determined experimentally to those calculated from equation [15], using both the value of H determined from equation [8] and a value reported by Spanner (8).

Source of experimental data	Thermocouple wire length	Thermocouple wire radius	Experimentally determined cooling current	Calculated cooling current	
				$H = 83.31 \times 10^{-4}$ Eq. [8]	$H = 12.4 \times 10^{-4}$ Spanner (8)
	cm	cm	ma.	ma.	ma.
Monteith and Owen (5)	0.8	0.008	30	55.9	40.7
Brix and Kramer*	0.8	0.005	20	25.5	16.6
Box (1)	0.8	0.004	15	17.8	10.9
Lambert and van Schilfgaarde (4)	**	(0.004)	35		
Rawlins and Dalton (6)	0.8	0.00127	3	3.0	1.4
Campbell et al. (2)	0.2	0.00127	5	4.6	3.9

*Personal communication from Holger Brix and Paul J. Kramer.

**Length of thermocouple not reported. Assuming the wire radius to be 0.004 cm, from Figure 2 the length for optimum cooling using 35 ma. would be approximately 0.25 cm.

radius increases, however, the experimentally determined cooling currents are significantly less than the calculated values. This deviation probably occurs because heat sinks at the reference junctions of these thermocouples were not sufficiently large to dissipate fully the heat generated with such high cooling currents. When this boundary condition is not met, the experimentally determined optimum cooling current will be less than that calculated.

Heat Sink Requirements

To maintain the boundary condition of no temperature change at the reference junction, there will be varying heat sink requirements depending on the size of the thermocouple wire and the magnitude of the cooling current. To determine the heat sink requirements to a first approximation, we can consider the following.

When a cooling current is being passed through the thermocouple wires, the same quantity of heat being absorbed at the sensing junction is being generated at the reference junction. Thus, the total mass of material required to dissipate the heat generated by the Peltier effect, such that the change in temperature, ΔT, is given by

$$m = \frac{P i t}{C \Delta T} \qquad [17]$$

where m is the mass of the heat sinks, i is the current, t is the time that the current is flowing, C is the specific heat of the heat sink material and ΔT is the allowed temperature change. To maintain this junction as a reference junction, we shall require that its temperature not change more than 0.001°C.

With the assumption that the heat sink material has very high thermal conductivity, the magnitude of the cooling current and the time that it is allowed to flow uniquely determine the heat sink requirement. Figure 3 shows the mass of copper required to meet the above criteria as a function of the magnitude of the cooling current. For example, a thermocouple psychrometer using 0.008 cm radius (6.3 mil diam.) wire and an optimum cooling current of 56 ma. for 60 seconds would require a copper heat sink with a mass of about 150 grams. If the heat sink requirements are not met, the optimum cooling current will be depressed and the thermocouple psychrometer will lose sensitivity due to the reduced temperature depression of the sensing junction. Also, the calibration of such psychrometers will show a positive voltage output at zero bars water potential.

SUMMARY AND CONCLUSIONS

The heat transport coefficient of fine wire thermocouples in moist air has been determined experimentally. This value, determined from one wire size, allowed the calculation of optimum cooling currents for thermocouple wires having a wide range of sizes. As a result of being able to predict the magnitude of the cooling current, one can also determine the heat sink requirement.

Where miniaturization is desired, one must resort to small cooling currents so that the heat sink requirements can be met with a minimum amount of material. This is easily accomplished with the use of fine wire thermocouples because of the small cooling currents required.

LITERATURE CITED

(1) Box, J. E., Jr. 1965 Chapter 11. Design and Calibration of a Thermocouple Psychrometer which Uses the Peltier Effect. In Humidity and Moisture, Arnold Wexler, Ed., Reinhold Publ. Corp., New York, N.Y., Vol. I, Principles and Methods of Measuring Humidity in Gases, pp. 110-121.

(2) Campbell, G. S., Zollinger, W. D., and Taylor, S. A. 1966 Sample changer for thermocouple psychrometers: Construction and some applications. Agron. J. 58: 315-318.

(3) Carslaw, H. S., and Jaeger, J. C. 1947 Conduction of Heat in Solids. Oxford Press, London.

(4) Lambert, Jerry R., and van Schilfgaarde, Jan. 1965 A method of determining the water potential of intact plants. Soil Sci. 100: 1-9.

(5) Monteith, J. L., and Owen, P. C. 1958 A thermocouple method for measuring relative humidity in the range 95-100%. J. Sci. Instr. 35: 443-446.

(6) Rawlins, S. L., and Dalton, F. N. Psychrometric measurement of soil water potential without precise temperature control. (in preparation)

(7) Roeser, William F. 1940 Thermoelectric thermometry. J. Applied Phys. 11: 388-407.

(8) Spanner, D. C. 1951 The Peltier effect and its use in the measurement of suction pressure. J. Exptl. Bot. 2: 145-168.

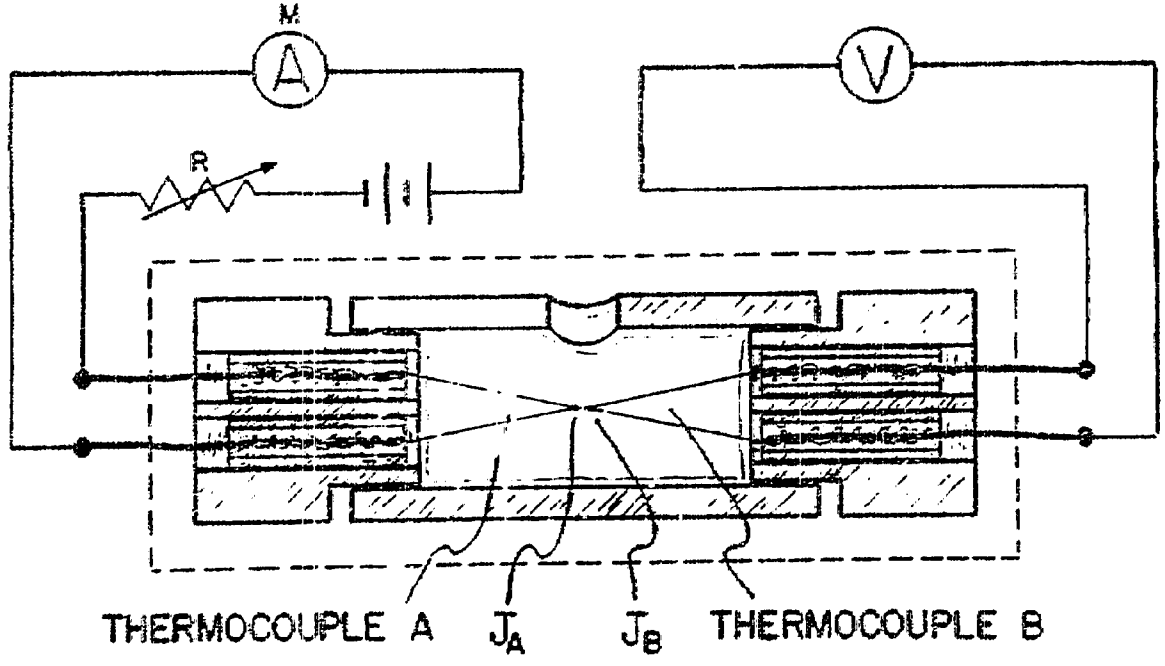

Figure 1.--Schematic representation of experimental setup used to determine the heat transport coefficient for Chromel-Constantan wires in moist air. Current through thermocouple A was adjusted to give zero temperature depression at J_a. Thermocouple B was used to measure the temperature depression at J_b.

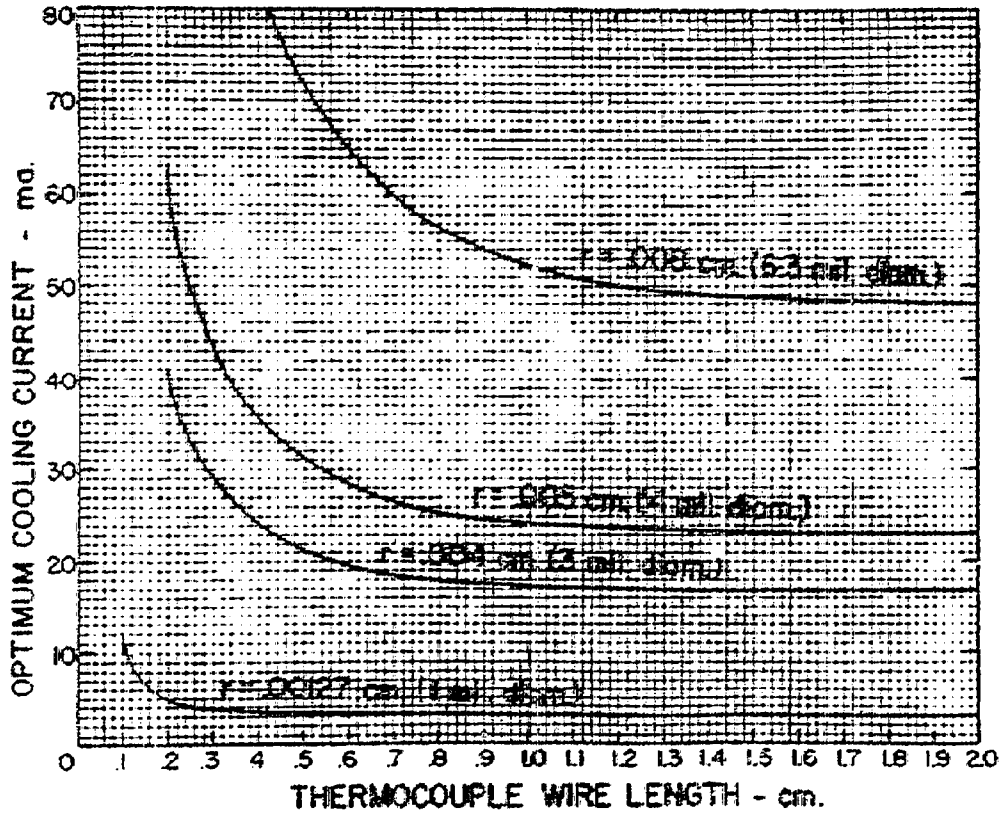

Figure 2.--Optimum cooling current as a function of thermocouple wire length for Chromel-Constantan thermocouples of various radii. Data were computed from equation [15].

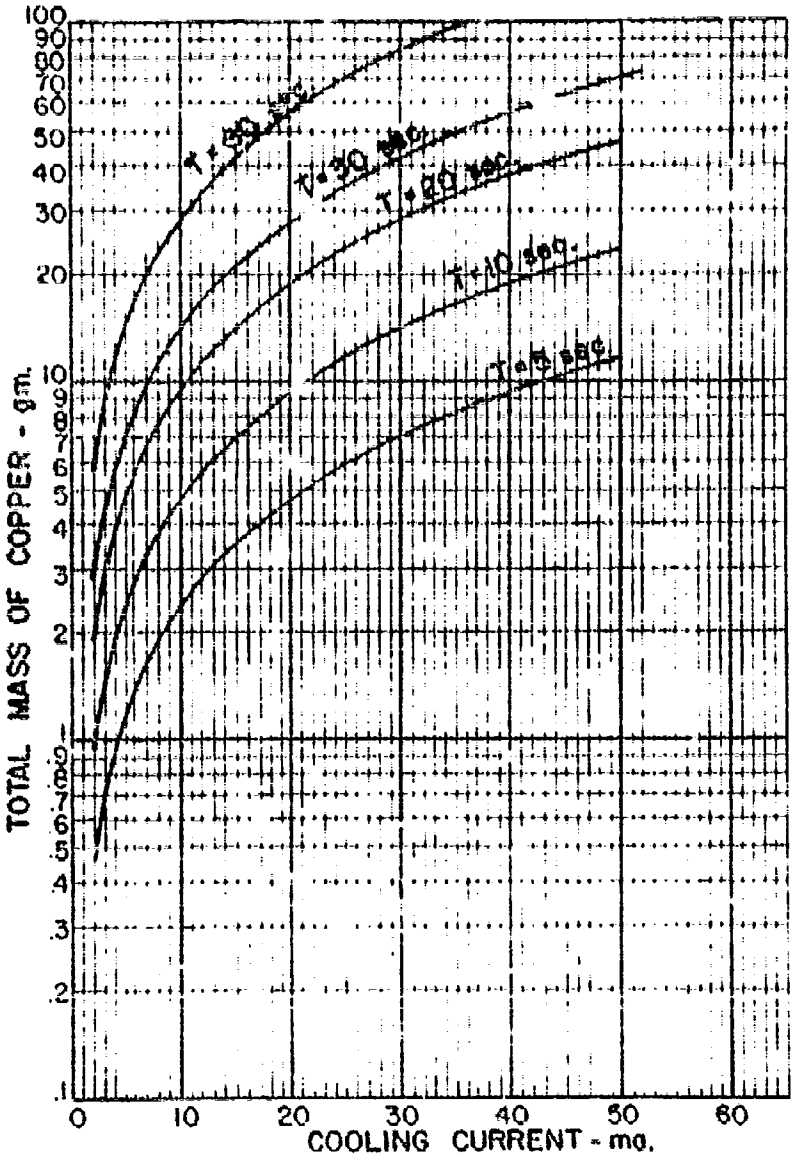

Figure 3.--Mass of copper at psychrometer heat sinks as a function of cooling current for various lengths of time the cooling current is applied. Data were computed from equation [17] assuming a temperature elevation at the heat sinks of 0.001°C.

EFFECT OF SOIL SALINITY ON WATER POTENTIALS AND TRANSPIRATION IN PEPPER (Capsicum frutescens)

C. F. Ehlig, W. R. Gardner and M. Clark

Agronomy Journal ___: ___-___, 196_.

APPENDIX C

EFFECT OF SOIL SALINITY ON WATER POTENTIALS AND TRANSPIRATION IN PEPPER (Capsicum frutescens)[1]

C. F. Ehlig[2], W. R. Gardner[2] and M. Clark

ABSTRACT

Total leaf water potential, osmotic potential, and turgor potential were measured on pepper plants irrigated with saline water having an osmotic potential of two bars. Results are compared with similar measurements on nonsaline treatments. Plants were allowed to extract water from the soil until the total water potential reached about -16 bars. Transpiration rate was also determined.

The difference between the leaf water potential and the soil water potential was the same for both treatments. The relation between the leaf water content and component water potentials was that predicted from the nonsaline leaves, assuming an osmotic adjustment in the saline leaves of two bars. No further adjustment due to concentration of the soil solution was observed. The relative transpiration rate was reduced at a much higher soil water content for the saline than for the nonsaline case.

---

[1]Contribution from the U. S. Salinity Laboratory, Soil and Water Conservation Research Division, Agricultural Research Service, USDA, Riverside, Calif. 92502. This work was supported in part by the Atmospheric Sciences Laboratory, Research Division, U. S. Army Electronics Command, Fort Huachuca, Arizona 85613.

[2]Present Address: U. S. Plant, Soil and Nutrition Laboratory, Tower Road, Ithaca, N.Y. 14850, and Department of Soils, University of Wisconsin, Madison, Wisconsin 53706, respectively.

As the potential energy of the soil water decreases due to water uptake by the plant, the water potential in the plant decreases accordingly. This is essential if water is to be taken up to replace that continually lost by transpiration. In previous papers (Gardner and Ehlig, 1962; Ehlig and Gardner, 1964; and Gardner and Ehlig, 1963), we reported results of studies verifying that the water potential in the plant leaf could be related to that in the soil according to the passive model of water transport in which the flux of water in the soil-plant system is assumed to be proportional to the water potential gradient. In the previous studies, the decrease in soil water potential was due entirely to the adsorption forces in the soil giving rise to the matric potential. When salts are present in the soil solution, they also lower the potential energy of the water, and according to the theory of water uptake, the decrease in plant water potential should be the same for a given decrease in soil water potential, whether this decrease is in the matric or osmotic component, or both. This assumes that the resistance of the system remains unchanged. The plant leaf water potential is also made up of two major components, i.e., the osmotic and the turgor potentials. If the salts were completely excluded from the plant, the decrease in leaf water potential resulting from a decrease in soil water potential should be the same for the saline as for the nonsaline case. However, it has been observed (Bernstein, 1961) that an osmotic adjustment occurs in many plants when they are grown in saline media. Bernstein (1963) found that in young bean plants this

adjustment occurred rather rapidly and corresponded almost exactly to the change in the osmotic potential of the solution in which the plants were growing. On the other hand, pepper plants exhibited a much slower and less complete adjustment. Inasmuch as the salinity of the soil solution fluctuates under field conditions, the dynamics of this adjustment may have an influence on the response of the plant to salinity.

This paper presents results of a study of the relation between the components of water potential in pepper plant to those in the soil as a function of time as the plant extracts water from a salinized soil. The relation of transpiration rate to soil water content and water potential was also investigated, and compared with the nonsaline case.

Materials and Methods

Individual pepper plants (Capsicum frutescence L. var. California Wonder) were grown in glazed crocks packed with Chino clay soil. Crocks were 22 cm in diameter and 36 cm deep. All plants were grown to test size in a greenhouse where temperatures varied between 20 C and 30 C. Each crock was periodically fertilized with inorganic salts and was irrigated when the total water potential was about -0.5 bars, except during the actual experimental tests. Deionized water was used for the nonsaline crocks. In the salinized crocks a solution with an osmotic potential of about -2.0 bars was applied from the seedling stage onward. This solution contained two parts Na to one each of Ca and Mg, with chloride as the anion. More than enough water was applied at each irrigation to leach out the salt applied in the previous irrigation.

In a preliminary test, plants were grown with deionized water until just before the actual test, when they were irrigated with the saline water. Since the results, insofar as the internal water relations of the plant leaves were concerned, were the same as for the plants grown under saline conditions from the seedling stage, only the latter results are reported. Tests were conducted while the plants were in the fruiting stage. At this stage, their total leaf surface remains relatively constant because the products of photosynthesis are utilized mainly for fruit production rather than vegetative enlargement. The plants were four to five months old at the time of the tests. Three plants from each treatment were used in the tests. These were placed in a controlled environment chamber three to five days before the tests were initiated, and irrigated at the beginning of the test. They were then allowed to remove water from the soil until they wilted severely.

During the experiment, night temperatures in the chamber were held between 23 and 25 C with day temperatures between 25 and 30 C. The relative humidity stayed between 40 and 60 %. Light intensity in the vicinity of the exposed leaf surfaces ranged between 2000 and 4000 foot candles, and the lights were on 12 hours each day.

Transpiration was determined by weighing the plants in their containers at the beginning of each photoperiod. Plant leaves were collected daily about three hours after the start of a photoperiod. The total water potential and the osmotic potential were measured on the same sample from an individual leaf with the thermocouple psychrometer as previously described by Ehlig (1962). The relative water content was determined on discs or sections from the same leaf.

Soil samples were collected from the 10 to 15 cm depth just prior to the time of collection of the plant leaf samples. The water potential of each sample was determined using the psychrometric procedure described by Richards and Ogata (1958). The water content of each sample was determined by oven drying at 110 C immediately after its total water potential had been measured. Any large roots in the sample were removed before the water content measurement. The dry soil samples were extracted with distilled water, 1:1 by weight. Suspended particles were removed from the soil solution by centrifugation after which the osmotic potential of the solution was determined psychrometrically.

Results and Discussion

The relation between the soil water content and the water potential for both the saline and the nonsaline cases is shown in Fig. 1. These results are in agreement with those of Richards and Ogata (1961), in that the total potential equals the sum of the osmotic and matric potential, and the latter depends only on the water content of the soil. The osmotic potential at the highest soil water content is essentially that of the irrigation water. At lower water contents the osmotic potential decreases in proportion to the increasing concentration of the soil solution. No precipitation of salts was expected or observed. At 40 % water content by weight, most of the total water potential is due to the osmotic potential in the saline case. At the lowest water content, about 19 % by weight, the total potential of -16 bars was made up of components of -10 bars osmotic and -6.0 bars matric.

Fig. 1

The water content is plotted as a function of time in Fig. 2. The initial transpiration rate was somewhat higher for the nonsaline than for the saline treatment because of the larger size of the nonsaline plants. The transpiration rate relative to the initial transpiration rate for the nonsaline treatment is plotted as a function of soil water content in Fig. 3. The curves in Figs. 2 and 3 are smoothed so they do not reflect the diurnal fluctuations in the transpiration rates.

Fig. 2

Fig. 3

The relation between the plant leaf water potential and the soil water potential is shown in Fig. 4. The triangles represent the data for the saline treatment and the circles those for the nonsaline treatment. There is somewhat more scatter in the data for the salinized plants, but for both treatments the leaf water potential remained consistently about 2.5 bars lower than the soil water potential. This difference in potential is largely determined by the resistance to water movement through the plant and the transpiration rate. There is no <u>a priori</u> reason to expect it to remain constant. Apparently the decrease in transpiration rate at the lower water contents just compensated for the increase in resistance in the system.

Fig. 4

The lowering of the soil water potential due to the added salt in the saline treatments resulted in the predicted lowering of the osmotic potential in the plant leaves, when the leaves were relatively turgid. The relation between the plant water potential and the osmotic potential is shown in Fig. 5. The turgor potential, as obtained by taking the difference between the smooth curves through the data points

Fig. 5

and the straight line with the 45° slope in Fig. 5, is plotted against total water potential in Fig. 6. The increase in turgor potential due to the osmotic adjustment in the saline case compared with the nonsaline, persists and remains constant as the leaf water potential decreases until the turgor potential approaches zero. A corresponding change in the relation between the relative water content and the total water potential is also caused by the osmotic adjustment. For water potential values above about -10 bars, the relation between the potential and the leaf water content is essentially the same for the nonsaline and the saline cases as seen in Fig. 7. However, the marked break in the curve, which is associated with visible wilting, occurs at about -10.5 bars potential for the nonsaline case and -14 for the saline. This corresponds to a turgor potential of about 1 bar in both cases. Both the nonsaline and the saline data fit the physical model described elsewhere by the authors (Gardner and Ehlig, 1965). In this model, the plant leaf tissue is assumed to behave as an ideal osmometer in which the elastic modulus of the cell walls has a relatively high, but constant, value at the higher turgor potentials and drops abruptly to a relatively low value as the turgor potential approaches zero. In this model, the solute content of the cells is assumed constant so that the concentration varies inversely with the relative water content of the tissue. The elastic modulus appears to be independent of the level of salinity imposed, so that the relation between the various components of the leaf water potential can be predicted completely if

this modulus is known and if the osmotic potential corresponding to zero total water potential is known.

Figure 8 shows the relation between the various osmotic potentials and the soil water content. This is particularly interesting because the osmotic potential in the leaves of the saline plants shows the expected shift of just over two bars corresponding to the osmotic potential in the saline treatment. But there was essentially no further decrease in the leaf osmotic potential until the soil water content was down to about 25%, even though the soil osmotic potential was decreasing continuously. The subsequent decrease in leaf osmotic potential can be completely accounted for by dehydration of the leaf tissue. The plant was apparently able to adjust osmotically to the initial, or minimum, level of salinity in the soil solution, but could not keep up with the change due to concentration of the soil solution. This failure to adjust further is consistent with Bernstein's findings for pepper (1963).

Fig. 8

The total leaf water potential, osmotic potential, and turgor potential are plotted as a function of time in Fig. 9. Because of the osmotic adjustment that occurred, the turgor potential for the saline and nonsaline treatments do not differ greatly. However, this slight difference is consistent with the timing of the decrease in transpiration rate. For the nonsaline case, the transpiration rate began to decrease between day four and five. For the saline case, this occurred about day three. In both cases, this corresponds to a turgor pressure

Fig. 9

of about 5 bars. This differs from the one bar value for Fig. 7 because of the difference between the instantaneous rate of transpiration and the 24-hour average rate.

Figure 10 shows the relative transpiration rate plotted as a function of total leaf water potential. In this graph, the transpiration rates for the saline and nonsaline treatments are plotted relative to their respective maximum rates. Figure 11 shows the relative transpiration rate as a function of the turgor potential. Included in this figure are data from the preliminary experiment (experiment I) in which the plants were salinized just prior to the actual experiment. Whatever difference there may be between the data for saline and nonsaline treatments is obscured by the scatter in the data.

Conclusions

The results give encouraging support for the re , simple model for water uptake by plants and for the model relating the leaf water content to the components of the water potential, at least as a first approximation. From these models, given the relation between the turgor pressure and the transpiration rate, the water retention properties of a soil, and the initial salinity of the soil solution, it should be possible to predict the soil water content and the various components of the soil and plant water potential as a function of time. This, of course, does not answer the larger question of how the various components of the leaf water potential influence plant growth. If some of the empiricism can be eliminated from the correlations between soil salinity and plant growth this question should become that much more amenable to solution.

LITERATURE CITED

1. Bernstein, L. 1961. Osmotic adjustment of plants to saline media. I. Steady state. Am. J. Bot. 48: 909-918.

2. Bernstein, L. 1963. Osmotic adjustment of plants to saline media. II. Dynamic phase. Am. J. Bot. 50: 360-370.

3. Ehlig, C. F. 1962. Measurement of energy status of water in plants with a thermocouple psychrometer. Plant Physiol. ... 288-290.

4. Ehlig, C. F., and W. R. Gardner. 1964. Relationship between transpiration and the internal water relations of plants. Agron. J. 56: 127-130.

5. Gardner, W. R., and C. F. Ehlig. 1962. Impedance to water movement in soil and plant. Science 138: 522-523.

6. Gardner, W. R., and C. F. Ehlig. 1963. The influence of soil water on transpiration by plants. J. Geophys. Res. 68: 5719-5724.

7. Gardner, W. R., and C. F. Ehlig. 1965. Physical aspects of the internal water relations of plant leaves. Plant Physiol. 40: 705-710.

8. Richards, L. A., and Gen Ogata. 1958. A thermocouple for vapor pressure measurement in biological and soil systems at high humidity. Science 128: 1089-1090.

9. Richards, L. A., and Gen Ogata. 1961. Psychrometric measurements of soil samples equilibrated on pressure membranes. Soil Sci. Soc. Am. Proc. 25: 456-459.

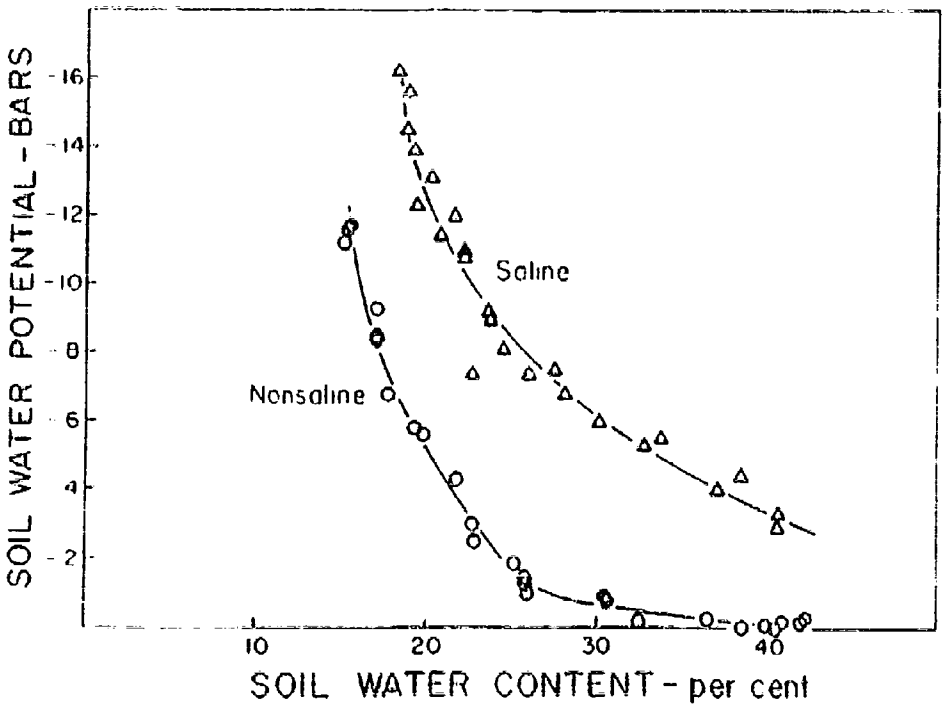

Figure 1.--Soil water potential as a function of soil water content. Deionized water or saline water (with an osmotic potential of -2.0 bars) was applied to Chino clay.

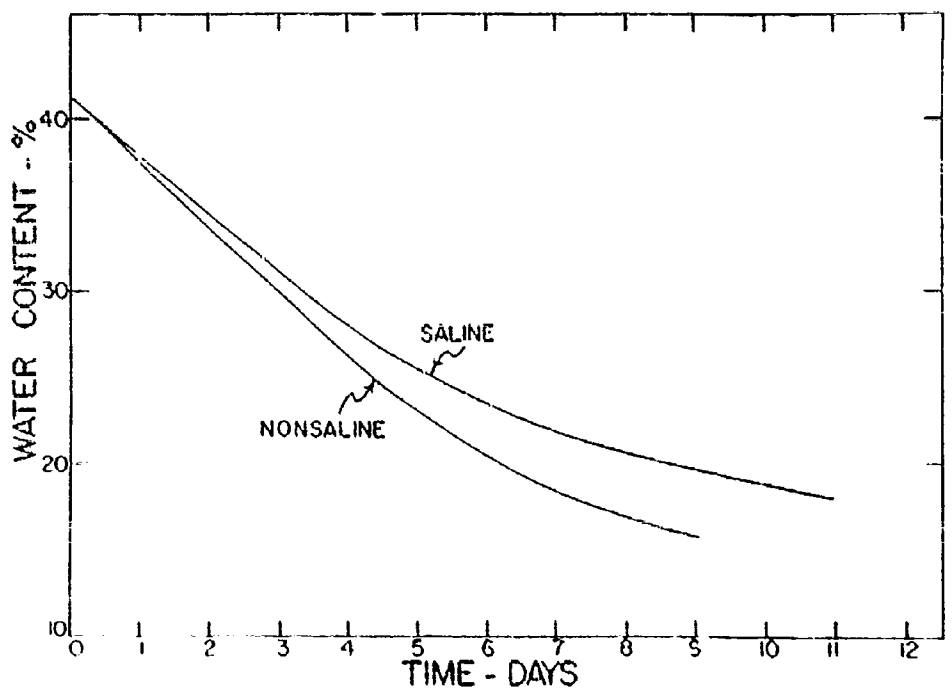

Figure 2.--Soil water content in percent by weight as a function of time.

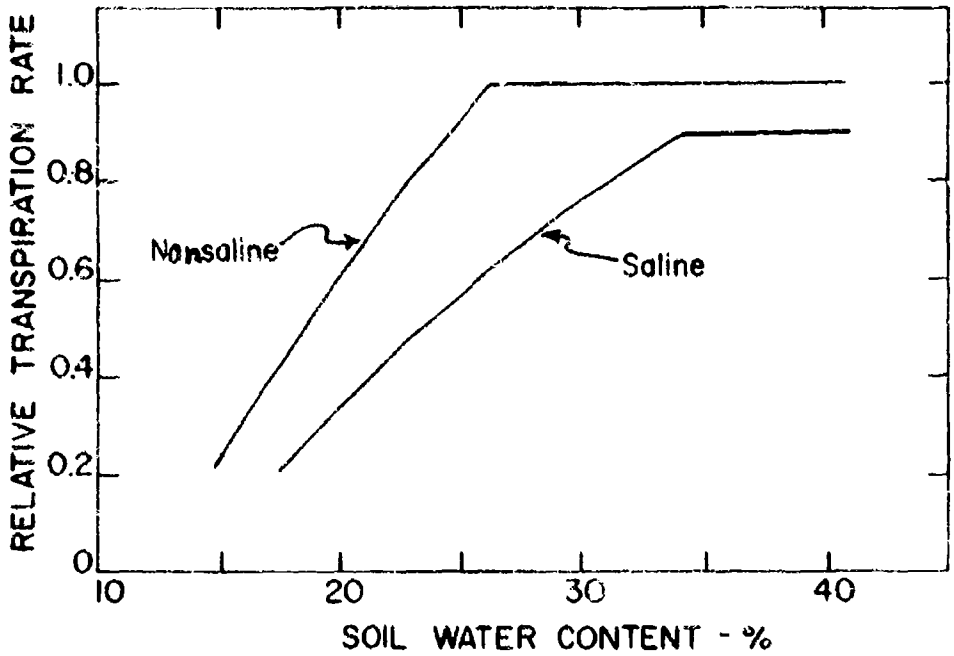

Figure 3.--Relative transpiration rate as a function of soil water content.

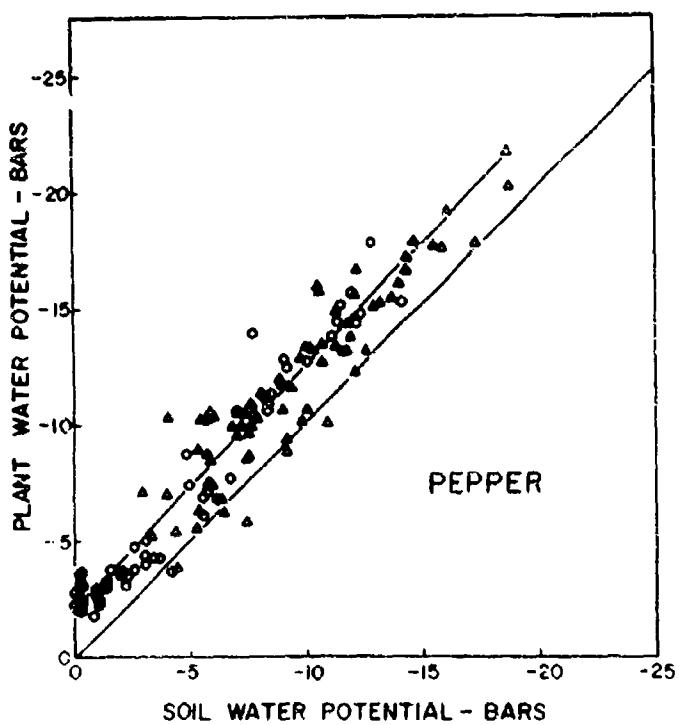

Figure 4.--Plant water potential as a function of total soil water potential. The circles represent the nonsaline treatment and the triangles the saline treatment.

GPO 827-851

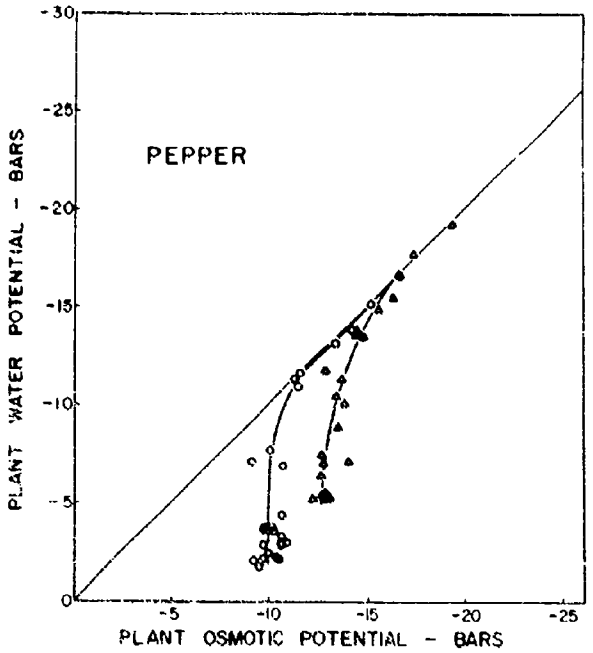

Figure 5.-- Plant leaf water potential (total) as a function of the osmotic potential component. The circles represent the nonsaline treatment and the triangles the saline treatment.

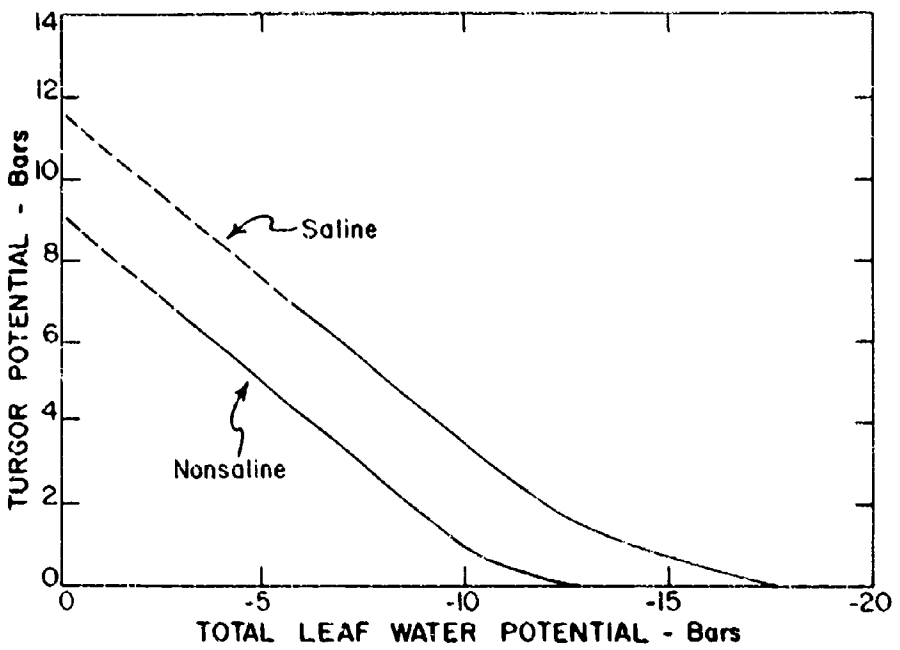

Figure 6.--Leaf turgor potential as a function of total leaf water potential for the saline and nonsaline treatments.

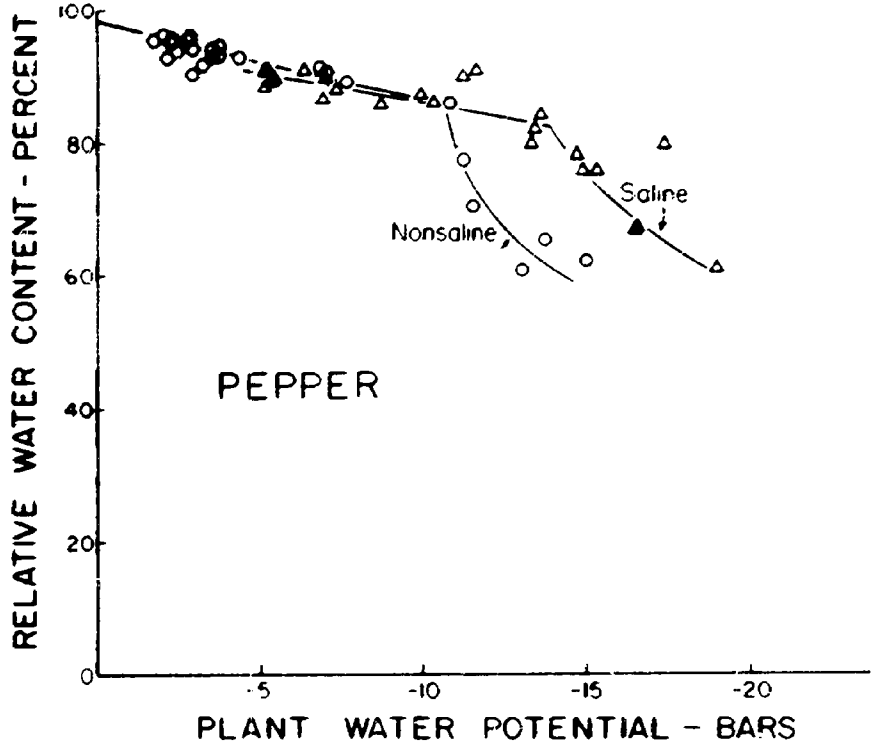

Figure 7.--Plant leaf relative water content as a function of total leaf water potential.

GPO 827-874

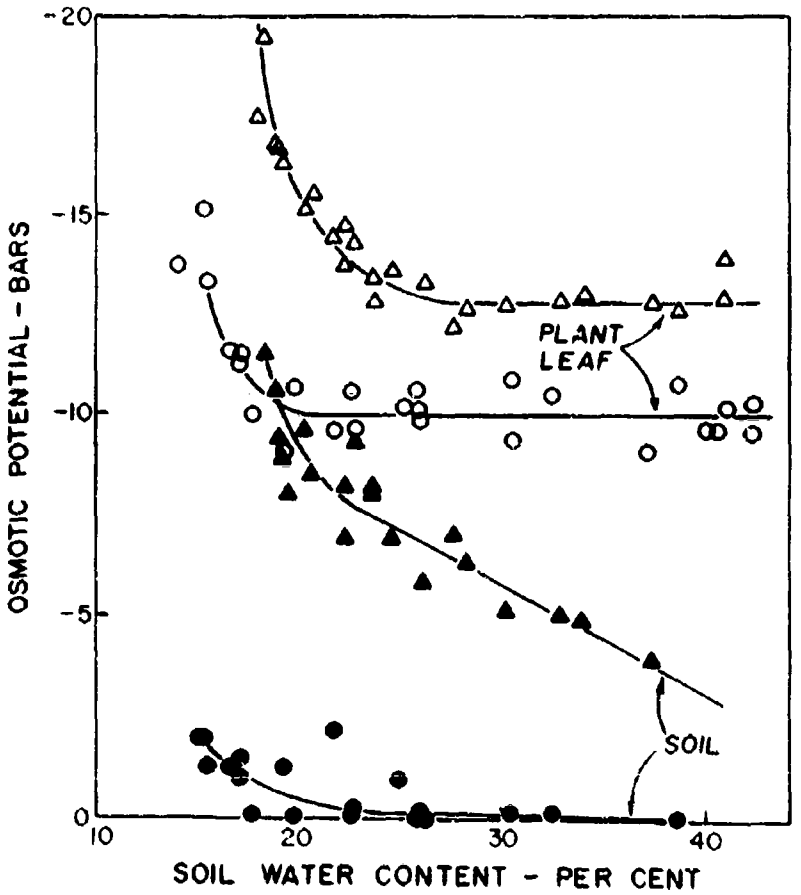

Figure 8.--The osmotic component of the soil and plant leaf water potential. The circles represent the nonsaline treatment and the triangles the saline treatment.

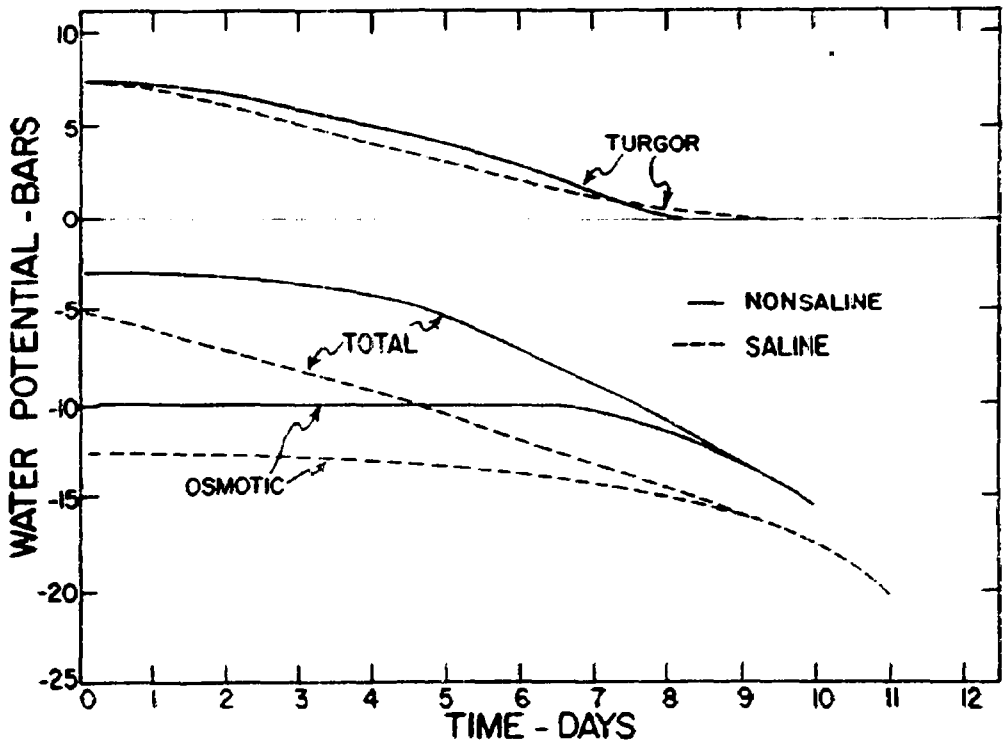

Figure 9.--The leaf water potential and its components as a function of time.

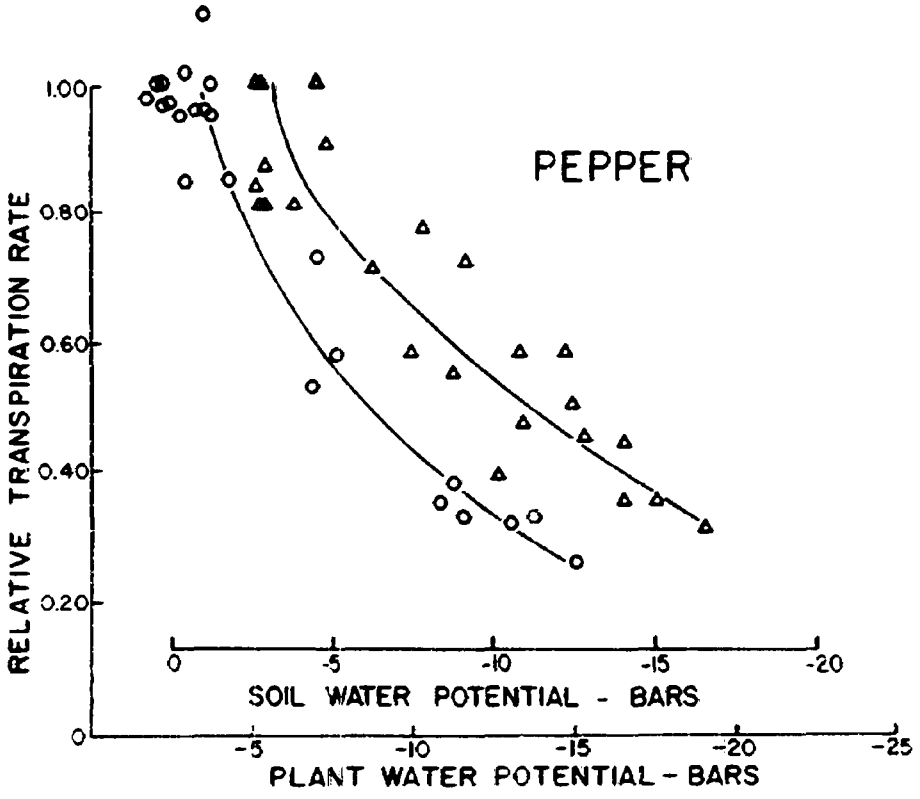

Figure 10.--Relative transpiration rate averaged over the 24-hour day plotted as a function of the total leaf and soil water potentials. The soil water potential is about 2.5 bars higher than the leaf water potential as seen in Fig. 2. The circles represent the nonsaline treatment and the triangles the saline treatment.

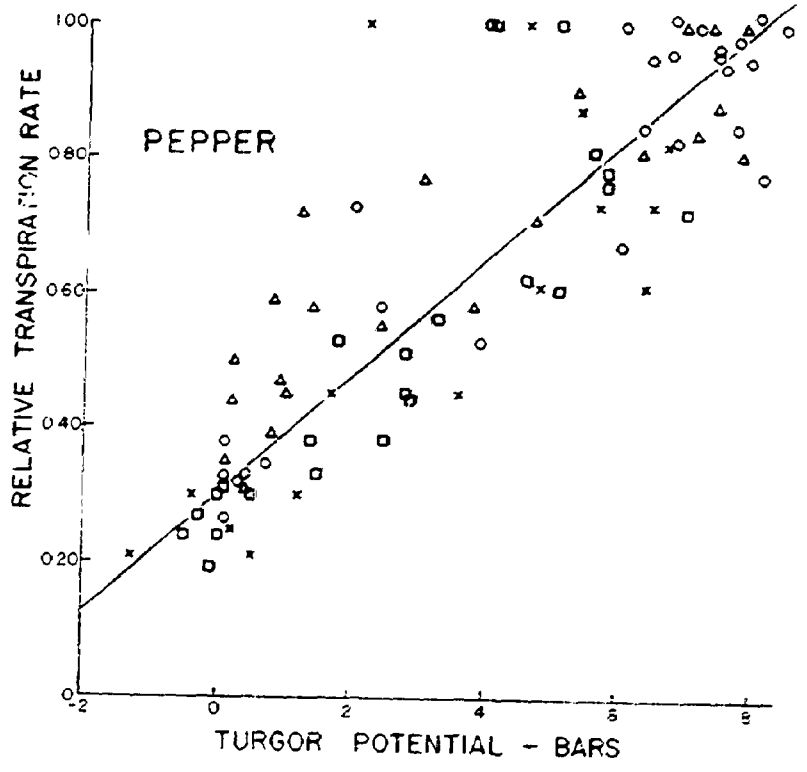

Figure 11.--Relative transpiration rate (24-hour average) plotted as a function of leaf turgor potential. The circles and triangles represent the data for the nonsaline and saline treatments, respectively, for the experiment in which the saline treatment was maintained continuously from the seedling stage. The crosses and squares represent the nonsaline and saline treatments, respectively, for the preliminary experiment in which the plants were salinized just prior to the experiment.

APPENDIX D

APPARATUS FOR WEIGHING THE LONG SOIL COLUMNS

E. J. Doering

APPARATUS FOR WEIGHING THE LONG SOIL COLUMNS

E. J. Doering

A device capable of detecting changes of the order of 10 grams in the weight of soil columns that weigh about 500 kilograms (1 part in 50,000) is needed for proposed greenhouse experiments. Commercially available mechanical weighing devices generally have a sensitivity of about 1 part in 1000, or, for this application, a sensitivity of the order of 400 to 500 grams. The cost of more sensitive mechanical devices increases quite rapidly, and the devices themselves are subject to higher maintenance requirements.

Hydraulic load cells have the advantage over mechanical devices in that they are simple and have no moving parts. Special attention, however, must be paid to membrane characteristics, temperature effects on fluids and materials, and methods for obtaining the desired reading. Bloeman describes a hydraulic load cell system for which he claims a sensitivity of 1 part in about 48,000. The unit was presumably put into use in 1963 at the Institute of Land and Water Management Research, Wageningen, The Netherlands. The apparatus described herein is similar in principle to Bloeman's (Transactions of Amer. Soc. Agr. Engrs. 7: 297-299, 1964) but with adaptations for use in the greenhouse where ambient temperatures diurnally fluctuate about 30 degrees Fahrenheit.

The Hydraulic Load Cells

A sketch of the cross-section of the hydraulic load cells is shown as Figure 1, and photographs of the completed components are shown as Figures 2 and 3. The microswitches that limit the lift so readings can always be made with the membrane at the same null position are shown attached to the top ring of the cell in Figures 2 and 3. The brass plate, D, in Figure 1 is not shown in the photographs because it is a part of the column base. In Figure 4, the cells are shown assembled and in place under the column.

From the dimensions shown in Figure 1, it is apparent that the membrane will be flat across and between the lower surfaces of the top ring, B, and the top plate, C, of the cell when the brass plate, D, has been lifted a distance of about 0.8 mm. (0.031 inch) from the top ring. This is the desired null position because the supporting surface for the column is then equal to the average of the areas of the lower surface of C and the hole in the bottom side of B. Less lift than this extends the effective membrane area to a larger lifting surface, and lifting above this null stretches the membrane so that it loses effective lifting surface. The 0.03-inch difference in thickness for plate C and ring B is not critical, however, as long as the difference is known.

The average measured effective membrane surfaces were found to be 134.2, 135.2, 133.8, 135.0, 134.5, and 134.8 cm^2 for completed cells numbered 1 through 6, respectively. Thus, for a total column weight of 500 kilograms, the working pressure will be 1240 grams/cm^2.

The Mylar polyester film provides the impermeable boundary for the oil in the cell, and the Fluorglas provides added strength. The ultimate strength of the membrane materials is not known, but fatigue is not expected to be a problem even under a constant load of 1240 grams/cm^2.

One-eighth-inch copper tubing was used to connect the cells to their respective manometer units to reduce the time required for the establishment of equilibrium between cell pressure and mercury pressure.

The Manometer Assembly

A sketch of the manometer wells is shown in Figure 5, and a photograph of the assembled manometer unit is shown as Figure 6. Because it is virtually impossible to center the load on these cells exactly, each cell has a separate mercury manometer. The three manometers are connected above the mercury, however, into a single readout manometer. The readout manometer is 1/8-inch precision bore glass tubing set on about a 2° incline so a change of 1 cm in the height of the mercury in any one of the half-inch diameter manometer tubes produces a change of 16 cm. in the position of the oil meniscus in the readout manometer. The dimension of the cells, the mercury wells, the manometer tubes, and the readout manometer are such that a change in weight of 683 grams for the column (1 cm of water on the soil surface) should produce about a 5-cm. change in the position of the oil meniscus in the readout manometer. Greater sensitivity can be obtained by either increasing the diameter of the manometer tubes or decreasing the diameter of the readout manometer.

Each manometer was charged with 135 ml. of filtered mercury. All air bubbles were removed from the manometer system during assembly by carefully manipulating the oil pressures in the cells and in the manometer assemblies.

Temperature Control

In order to achieve the desired precision of measurement of the weight changes for the columns, temperature control for the mercury manometers and the readout oil manometer is essential. The temperature coefficients of thermal expansion for glass, copper, oil, and mercury are all different, and a rising temperature produces a reading that is in error by being too large.

Temperature control for the mercury manometers in the water bath is achieved by the use of a Hallikainen Instruments Thermotrol unit (Shell Development Design, Patent No. 2838644). The heating coils have a capacity of about 600 watts. Rapid stirring is provided by a 6-inch-diameter centrifugal pump driven at 1725 revolutions per minute. The pump intake is at the bottom of the bath (because the water was giving up heat to the surroundings). The bath is insulated with two layers of foil-backed fiberglass bat to minimize heat loss.

Temperature control for the copper tubing is achieved by fastening the 3/16-inch copper tubes securely to a 1/2-inch copper and insulating the bundle with about a one-inch thickness of sponge rubber and insulation tape. Part of the temperature-controlled output of the circulating pump is forced through the 1/2-inch copper tube.

The return end of the 1/2-inch copper tube is encased in a plastic cylinder with the readout manometer and scales. So far, air has been used as the fluid to conduct heat from the copper to the glass, but the unit is sealed and can be filled with water (or some other fluid) if the need becomes evident.

Calibration

Tests were performed using volumetric water measurements and adding and removing solid weights. Both of these tests were done without evaporation taking place. The manometer readout tubes were read at approximately 3-minute intervals for intermittent 3-day periods. The change in position of the oil meniscus was plotted against change in weight of the soil column. Excellent results were obtained with a straight line being easily fitted. The resulting line varied slightly for columns A and B as shown in Figure 7.

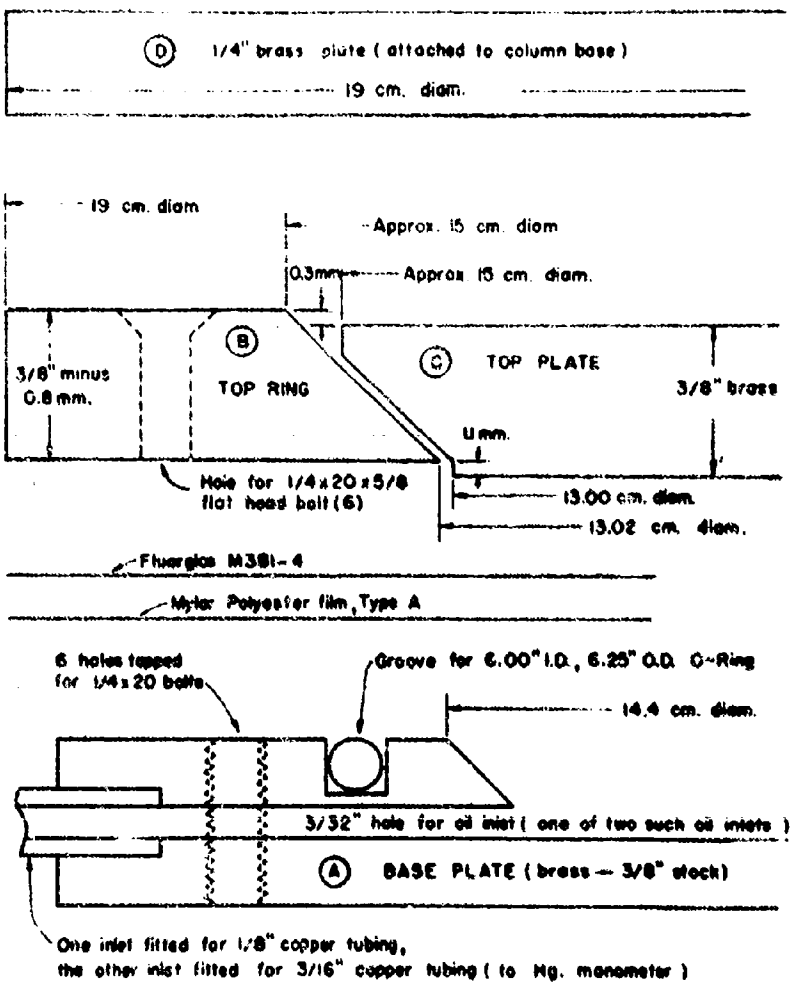

Figure 1.--Components of the hydraulic load cells.

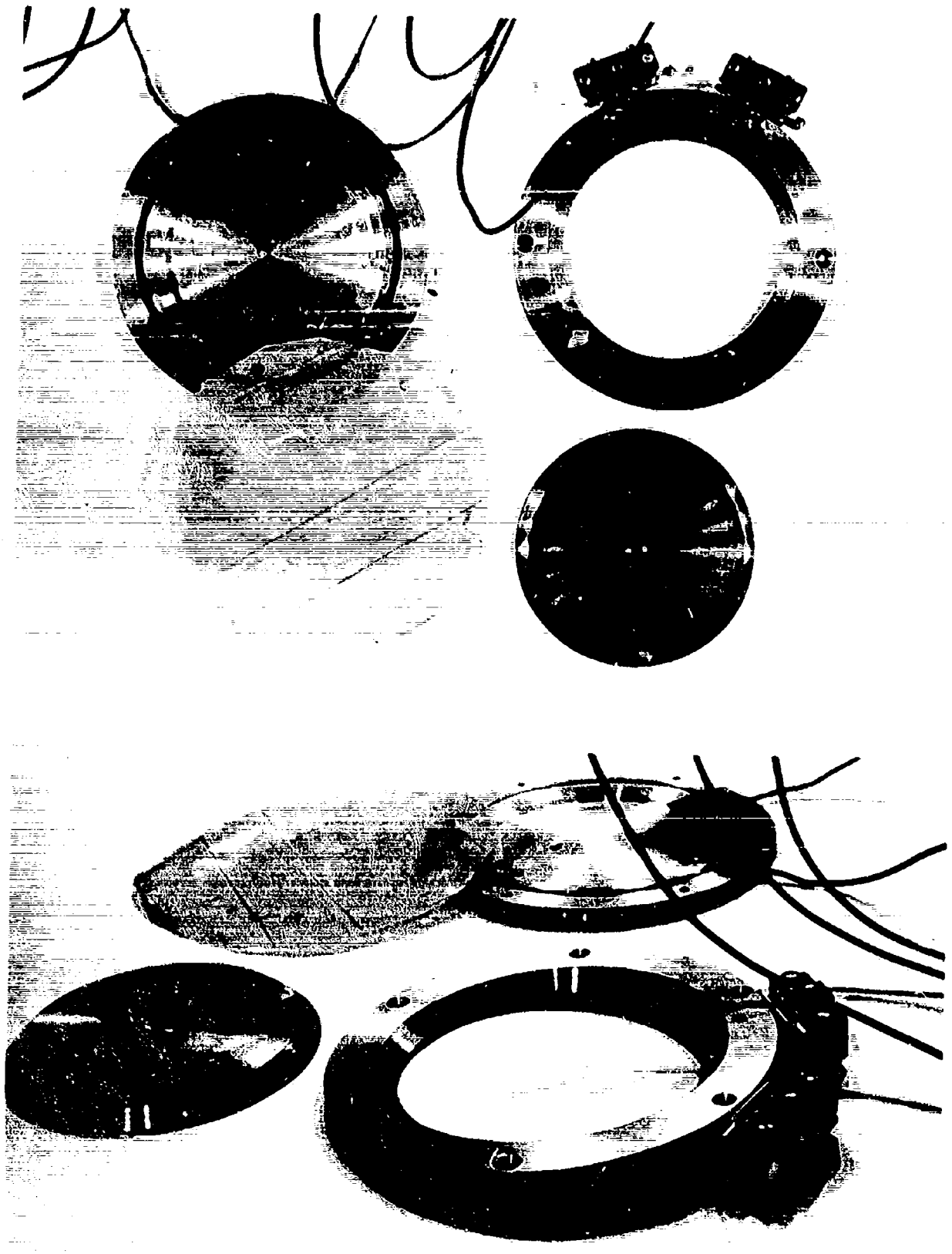

Figure 2.--Plan and oblique views of the components of the hydraulic load cells.

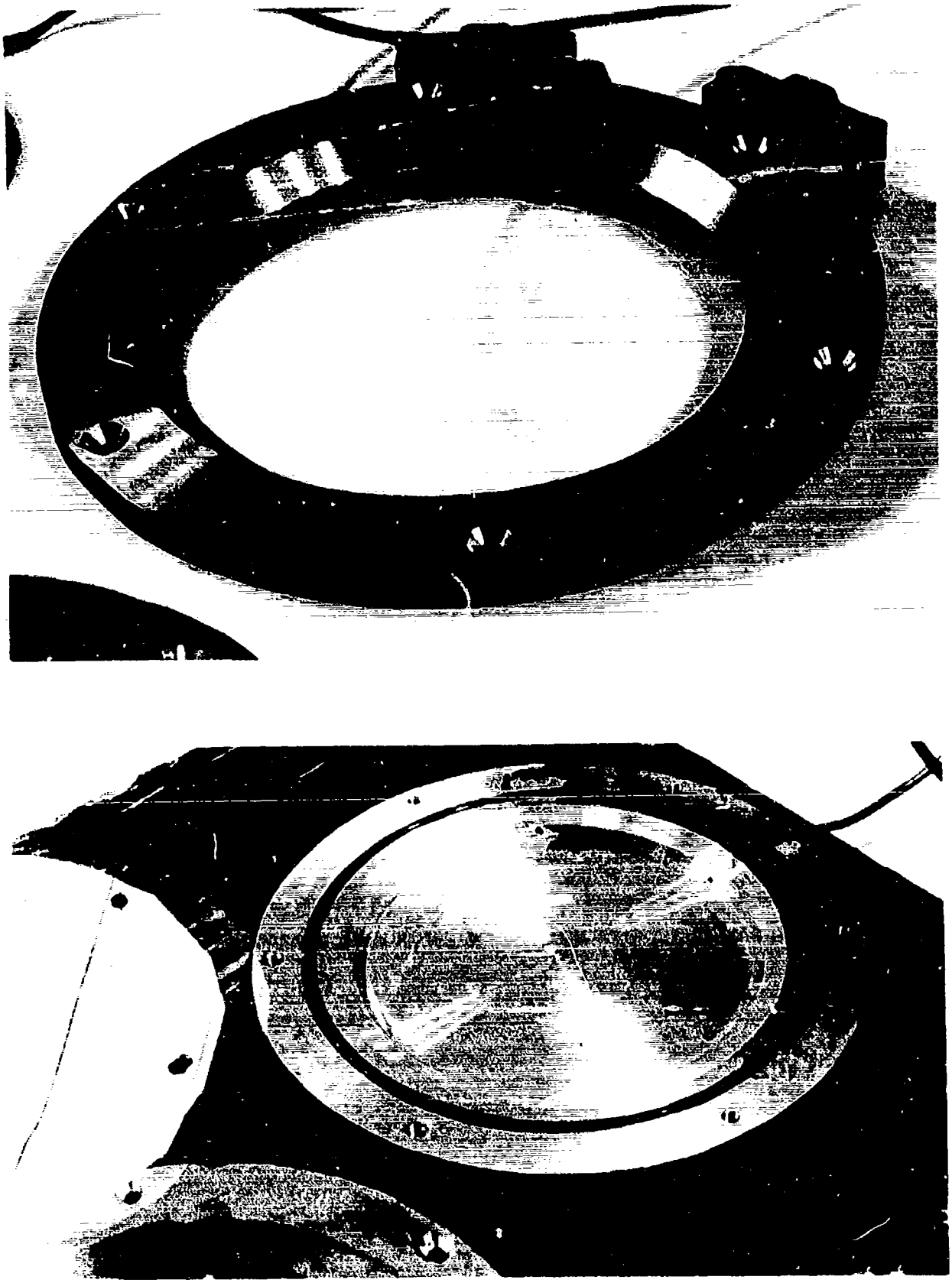

Figure 3.--Photographs of the top ring, B, and the base plate, A, for the hydraulic load cells.

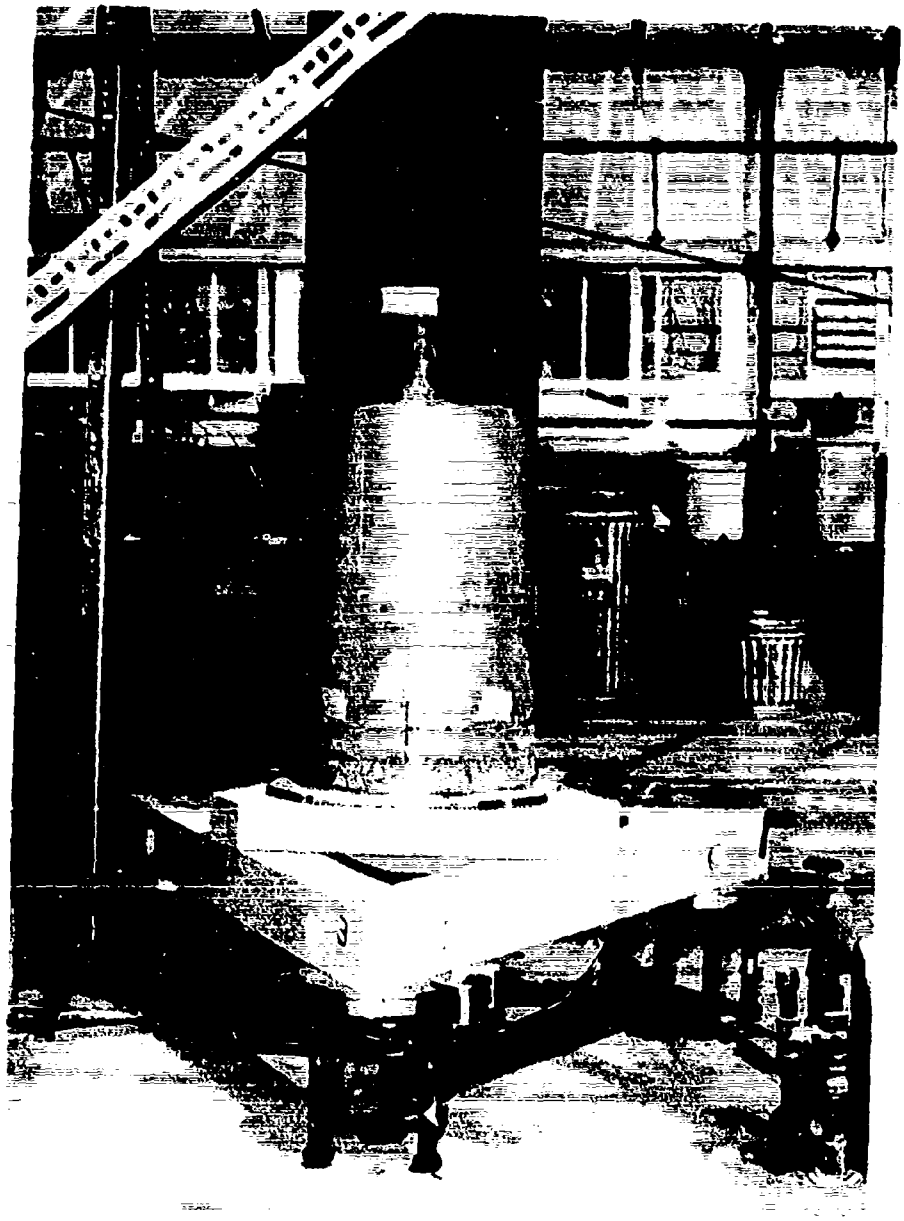

Figure 4.--Photograph of the hydraulic load cells in place under the triangular base of the south column.

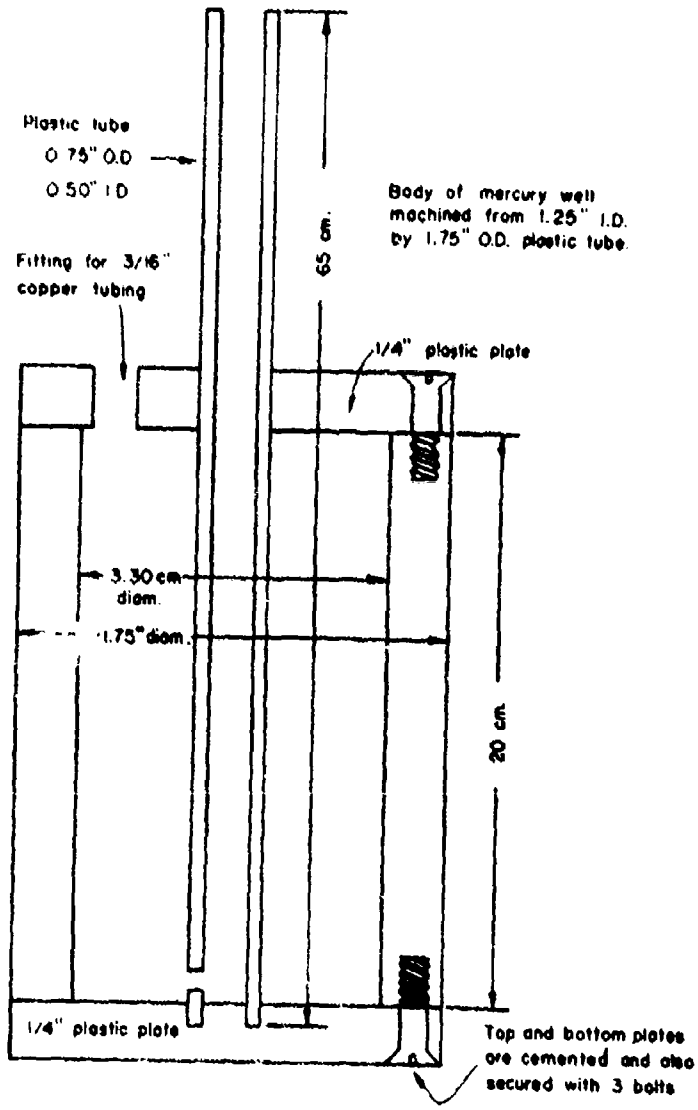

Figure 5.--Manometer assembly for each cell.

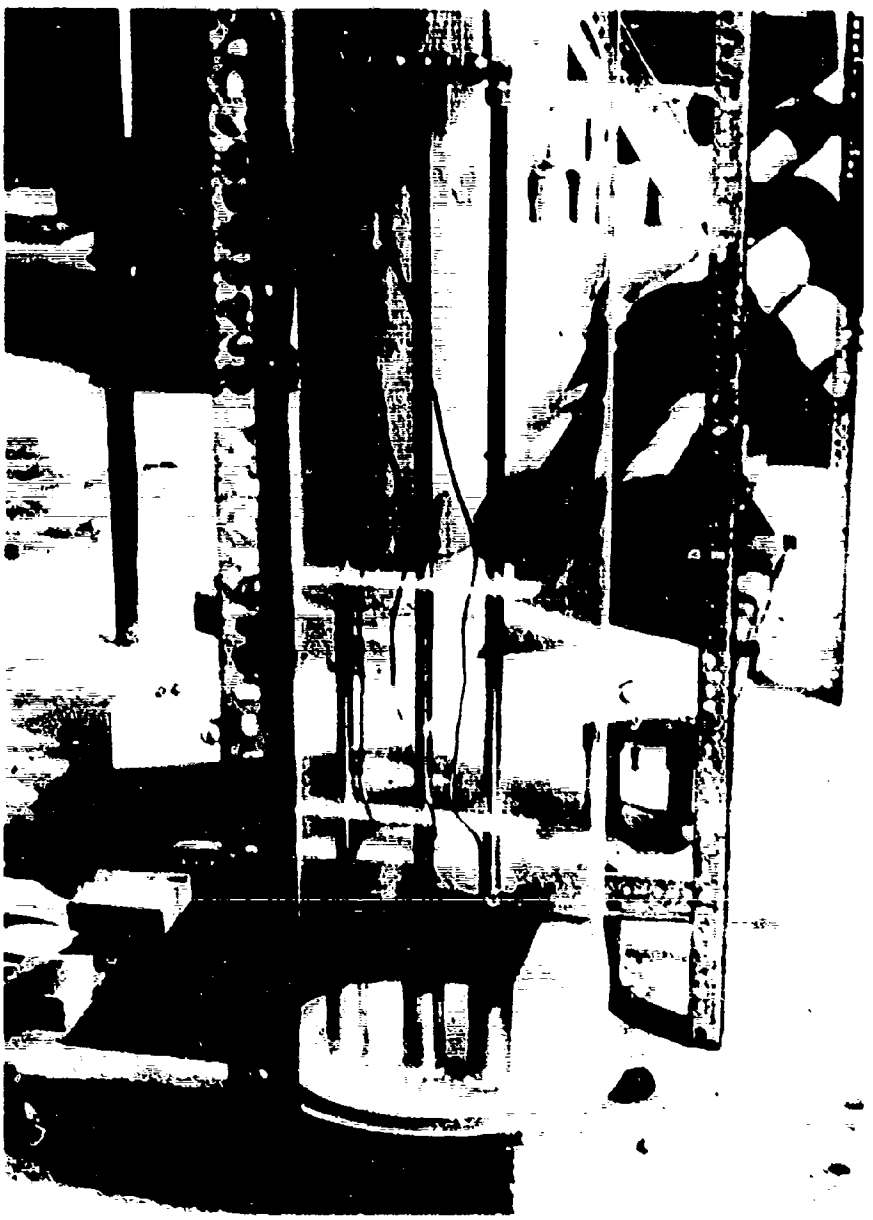

Figure 6.--Photograph of one of the completed manometer assemblies showing the connection of the three manometers above the mercury columns. (The copper lines to each manometer come from the load cells.)

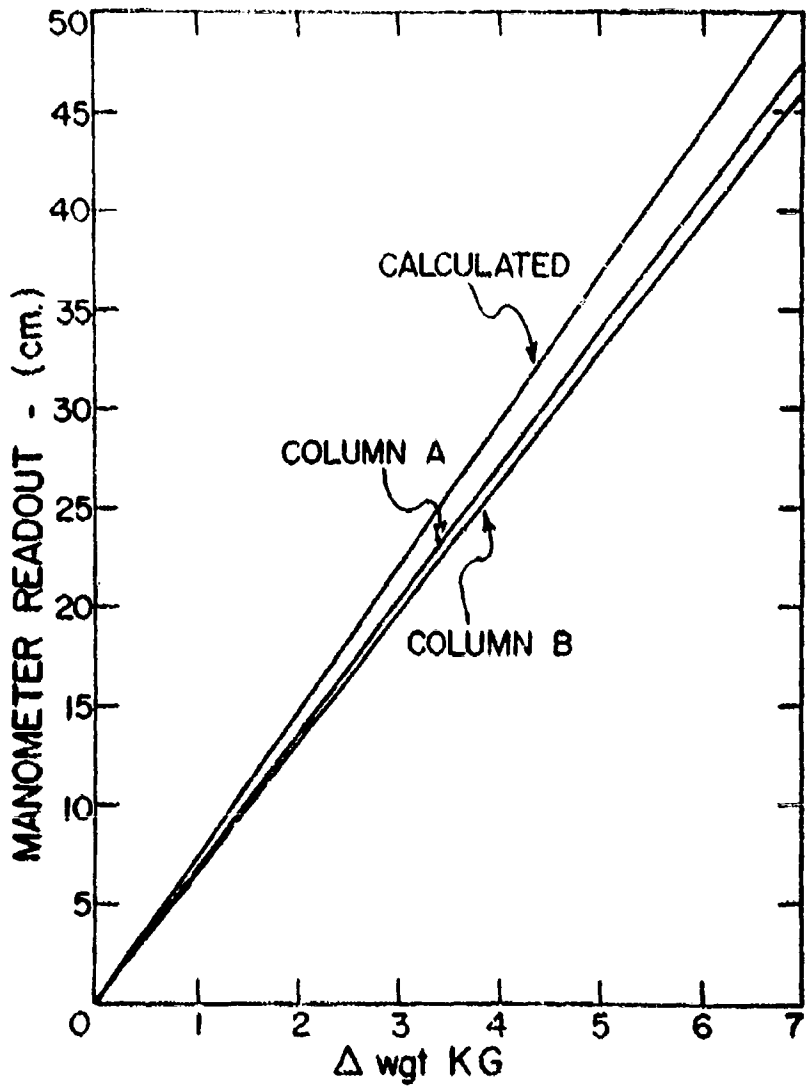

Figure 7.--Manometer readout as a function of weight added to soil columns A and B. The upper curve was calculated from manometer dimensions.

UNCLASSIFIED

Security Classification

DOCUMENT CONTROL DATA - R&D

(Security classification of title, body of abstract and indexing annotation must be entered when the overall report is classified)

1. ORIGINATING ACTIVITY (Corporate author)
U.S. Salinity Laboratory, Agricultural Research Service, Department of Agriculture, Riverside, California

2a. REPORT SECURITY CLASSIFICATION
Unclassified

2b GROUP

3. REPORT TITLE
WATER TRANSFER FROM SOIL TO THE ATMOSPHERE AS RELATED TO SOIL PROPERTIES, PLANT CHARACTERISTICS AND WEATHER

4. DESCRIPTIVE NOTES (Type of report and inclusive dates)
Annual report July 1965 to June 1966

5. AUTHOR(S) (Last name, first name, initial)
Rawlins, S. L., Gardner, W. R., Cullen, E. E., Dalton, F. N., Oster, J. D., Ingvalson, R. D., Enlig, C. F., Clark, M., and Doering, E. J.

6. REPORT DATE	7a. TOTAL NO. OF PAGES	7b. NO. OF REFS
December 1966	98	23

8a. CONTRACT OR GRANT NO.	9a. ORIGINATOR'S REPORT NUMBER(S)
Cross Service Order No. 2-66	
b. PROJECT NO.	
c. Task No. 1V0-14501-B53A-08	9b. OTHER REPORT NO(S) (Any other numbers that may be assigned this report)
d.	ECOM 2-66R-A

10. AVAILABILITY/LIMITATION NOTICES
Qualified requesters may obtain copies of this report from Defense Documentation Center, Cameron Station, Alexandria, Virginia 22314. Foreign announcement and dissemination of this report by DDC is not authorized.

11. SUPPLEMENTARY NOTES	12. SPONSORING MILITARY ACTIVITY
	U.S. Army Electronics Command Atmospheric Sciences Laboratory, Research Division, Fort Huachuca, Arizona

13. ABSTRACT Application of the theory for thermocouple psychrometers developed in last year's report has led to construction of psychrometers that essentially eliminates the requirement for precise temperature control. ~~Psychrometers of this type~~ were used to instrument a soil-plant system, and preliminary data on the influence of soil-water potential on transpiration rate were collected.

In ~~another experiment~~, a single pepper plant was grown in each of two soil columns 30 cm in diameter and 260 cm deep. A water table was set up in column A and the amount of water taken up from the water table was monitored daily. Column A received an amount of water approximately equal to 85% of that transpired since the previous irrigation. Column B received water equal to about 115% of the amount transpired. Soil water suction measurements were made daily with tensiometers placed at 50-cm depth intervals and at the 25-cm depth in the columns. Transpiration from the columns was determined daily by means of a load cell weighing system. Mathematical analysis of the data has not been completed, but an outline of the approach is given. It is apparent that attempts to estimate transpiration by means of soil moisture measurements will be in error if no way is provided to account for the flux of water into or out of the root zone.

The report includes the following chapter topics: plant-soil-water energy relations; water movement in the soil and uptake by plant roots; and further tests of the salinity sensor. Appendixes deal with psychrometric measurement of soil water potential without precise temperature control; design criteria for Peltier-effect thermocouple psychrometers; effect of soil salinity on water potentials and transpiration in pepper; and apparatus for weighing the long soil columns.

DD FORM 1 JAN 64 1473

UNCLASSIFIED

Security Classification

14. KEY WORDS	LINK A		LINK B		LINK C	
	ROLE	WT	ROLE	WT	ROLE	WT
Soil moisture transfer Soil moisture measurement Evapotranspiration Thermocouple psychrometer Soil water potential Hydraulic head Soil water diffusivity Soil salinity sensor						

INSTRUCTIONS

1. ORIGINATING ACTIVITY: Enter the name and address of the contractor, subcontractor, grantee, Department of Defense activity or other organization *(corporate author)* issuing the report.

2a. REPORT SECURITY CLASSIFICATION: Enter the overall security classification of the report. Indicate whether "Restricted Data" is included. Marking is to be in accordance with appropriate security regulations.

2b. GROUP: Automatic downgrading is specified in DoD Directive 5200.10 and Armed Forces Industrial Manual. Enter the group number. Also, when applicable, show that optional markings have been used for Group 3 and Group 4 as authorized.

3. REPORT TITLE: Enter the complete report title in all capital letters. Titles in all cases should be unclassified. If a meaningful title cannot be selected without classification, show title classification in all capitals in parenthesis immediately following the title.

4. DESCRIPTIVE NOTES: If appropriate, enter the type of report, e.g., interim, progress, summary, annual, or final. Give the inclusive dates when a specific reporting period is covered.

5. AUTHOR(S): Enter the name(s) of author(s) as shown on or in the report. Enter last name, first name, middle initial. If military, show rank and branch of service. The name of the principal author is an absolute minimum requirement.

6. REPORT DATE: Enter the date of the report as day, month, year; or month, year. If more than one date appears on the report, use date of publication.

7a. TOTAL NUMBER OF PAGES: The total page count should follow normal pagination procedures, i.e., enter the number of pages containing information.

7b. NUMBER OF REFERENCES: Enter the total number of references cited in the report.

8a. CONTRACT OR GRANT NUMBER: If appropriate, enter the applicable number of the contract or grant under which the report was written.

8b, 8c, & 8d. PROJECT NUMBER: Enter the appropriate military department identification, such as project number, subproject number, system numbers, task number, etc.

9a. ORIGINATOR'S REPORT NUMBER(S): Enter the official report number by which the document will be identified and controlled by the originating activity. This number must be unique to this report.

9b. OTHER REPORT NUMBER(S): If the report has been assigned any other report numbers *(either by the originator or by the sponsor)*, also enter this number(s).

10. AVAILABILITY/LIMITATION NOTICES: Enter any limitations on further dissemination of the report, other than those imposed by security classification, using standard statements such as:

(1) "Qualified requesters may obtain copies of this report from DDC."

(2) "Foreign announcement and dissemination of this report by DDC is not authorized."

(3) "U. S. Government agencies may obtain copies of this report directly from DDC. Other qualified DDC users shall request through _____."

(4) "U. S. military agencies may obtain copies of this report directly from DDC. Other qualified users shall request through _____."

(5) "All distribution of this report is controlled. Qualified DDC users shall request through _____."

If the report has been furnished to the Office of Technical Services, Department of Commerce, for sale to the public, indicate this fact and enter the price, if known.

11. SUPPLEMENTARY NOTES: Use for additional explanatory notes.

12. SPONSORING MILITARY ACTIVITY: Enter the name of the departmental project office or laboratory sponsoring *(paying for)* the research and development. Include address.

13. ABSTRACT: Enter an abstract giving a brief and factual summary of the document indicative of the report, even though it may also appear elsewhere in the body of the technical report. If additional space is required, a continuation sheet shall be attached.

It is highly desirable that the abstract of classified reports be unclassified. Each paragraph of the abstract shall end with an indication of the military security classification of the information in the paragraph, represented as *(TS), (S), (C), or (U).*

There is no limitation on the length of the abstract. However, the suggested length is from 150 to 225 words.

14. KEY WORDS: Key words are technically meaningful terms or short phrases that characterize a report and may be used as index entries for cataloging the report. Key words must be selected so that no security classification is required. Identifiers, such as equipment model designation, trade name, military project code name, geographic location, may be used as key words but will be followed by an indication of technical context. The assignment of links, rules, and weights is optional.